Synthesis and application of molybdenum based catalyst for oxidation reactions

Mihalinec, Josipa

Master's thesis / Diplomski rad

2019

University of Zagreb

FACULTY OF SCIENCE
Department of Chemistry

Josipa Mihalinec

SYNTHESIS AND APPLICATION OF MOLYBDENUM BASED CATALYST FOR OXIDATION REACTIONS

Diploma Thesis

submitted to the Department of Chemistry,

Faculty of Science, University of Zagreb

for the academic degree of Master in Chemistry

Zagreb, 2019

Acknowledgments

Table of Contents

University of Zagreb

Faculty of Science

Department of Chemistry

Diploma Thesis

ABSTRACT

SYNTHESIS AND APPLICATION OF MOLYBDENUM BASED CATALYST FOR
OXIDATION REACTIONS

Josipa Mihalinec

Synthesis of the dioxomolybdenum(VI) was carried out by using $[MoO_2(acac)_2]$ and the corresponding ONO hydrazone ligand (2,3-dihydroxbenzaldehyde isonicotinoylhydrazone, H_2L^1 or 2,3-dihydroxbenzaldehyde nicotinoylhydrazone, H_2L^2). Polynuclear complexes, $[MoO_2(L^1)]_n \cdot MeCN$ and $[MoO_2(L^2)]_n$ were obtained from acetonitrile, whereas mononuclear complexes $[MoO_2(L^{1,2})(MeOH)]$ were isolated from methanolic solution. The mechanochemical synthesis employing liquid assisted grinding was also applied, and H_2L^1 ligand and mononuclear complexes were obtained in such a way. *Ex-situ* powder X-ray diffraction method was implemented for monitoring H_2L^1 ligand obtained by mechanochemical synthesis. Complexes were characterized by IR spectroscopy, elemental and termogravimetric analysis. Additionally, polynuclear complexes were characterized by NMR spectroscopy. Molecular and crystal structures of H_2L^1 ligand and its mononuclear complex were determined by the single crystal X-ray diffraction. Lastly, the complexes were tested as catalyst in oxidation reactions of secondary alcohols, carveol and cyclohexanol by using H_2O_2 and TBHP (in aqueos solution or solution in decane).

(77 pages, 54 figures, 4 tables, 47 references, original in English)

Sveučilište u Zagrebu

Prirodoslovno-matematički fakultet

Kemijski odsjek

Diplomski rad

SAŽETAK

PRIPRAVA KOMPLEKSNIH SPOJEVA MOLIBDENA I NJIHOVA PRIMJENA KAO KATALIZATORA U REAKCIJAMA OKSIDACIJE

Josipa Mihalinec

U okviru ovog diplomskog rada pripravljeni su molibdenski(VI) kompleksi reakcijom $[MoO_2(acac)_2]$ i odgovarajućeg hidrazonskog liganda (2,3-dihidroksibenzaldehid izonikotinhidrazona, H_2L^1 ili 2,3-dihidroksibenzaldehid nikotinhidrazona, H_2L^2). Izolirani su polinuklearni $[MoO_2(L^1)]_n \cdot MeCN$ i $[MoO_2(L^2)]_n$ iz acetonitrila i mononuklearni kompleksi $[MoO_2(L^{1,2})(MeOH)]$ iz metanola. Ligand H_2L^1 i mononuklearne komplekse bilo je moguće sintetizirati mehanokemijski, mljevenjem potpomognuto kapljevinom. Osim toga, mehanokemijska sinteza liganda H_2L^1 je popraćena *ex-situ* metodom rentgenske difrakcije na polikristalnom uzorku. Kompleksi su identificirani IR spektroskopijom, elementnom i termogravimetrijskom analizom. Polinuklearni kompleksi karakterizirani su NMR spektroskopijom. Difrakcijom rentgenskog zračenja na monokristalnom uzorku je određena kristalna struktura H_2L^1 liganda te njegovog mononuklearnog kompleksa. Na kraju, pripravljeni kompleksi su ispitani kao katalizatori u reakcijama oksidacije sekundarnih alkohola, karveola i cikloheksanola u prisutnosti H_2O_2 i TBHP-a (u vodenoj otopini i otopini u dekanu).

(77 stranica, 54 slike, 4 tablice, 47 literaturnih navoda, jezik izvornika: engleski)

PROŠIRENI SAŽETAK

U ovom radu je bio poseban naglasak na primjeni principa zelene kemije (čišta, održiva sinteza s manje ili bez otapala, niska potrošnja energije i upotreba sigurnijih kemikalija) u svakom koraku istraživanja. Kako bi se slijedili principi zelene kemije, ideja je bila ispitati mogućnost dobivanja liganda i kompleksa mehanokemijskim putem, umjesto klasičnom sintezom u otopini te razviti ekološki prihvatljiv katalitički proces (mali udio katalizatora i upotreba tkz. zelenih oksidansa, H_2O_2 i TBHP-a)

Koristeći ekvimolarne količine 2,3-dihidroksibenzaldehida i odgovarajućeg hidrazida (izonikotin hidrazida ili nikotin hidrazida) klasičnom metodom u otopini pripravljeni su hidrazonski ligandi, 2,3-dihidroksibenzaldehid izonikotinhidrazon, H_2L^1 i 2,3-dihidroksibenzaldehid nikotinhidrazon, H_2L^2 (Slika 1).

Mehanokemijska sinteza mljevenjem potpomognuta kapljevinom (LAG) uspješno je provedena samo za ligand H_2L^1 pri 25 Hz, u trajanju od 60 min. Nastanak liganda je također popraćen je metodom difrakcije rentgenskog zračenja na polikristalnom uzorku. Iz difraktograma praha vidljiv je završetak reakcije i formiranje željenog produkta nakon 60 minuta mljevenja.
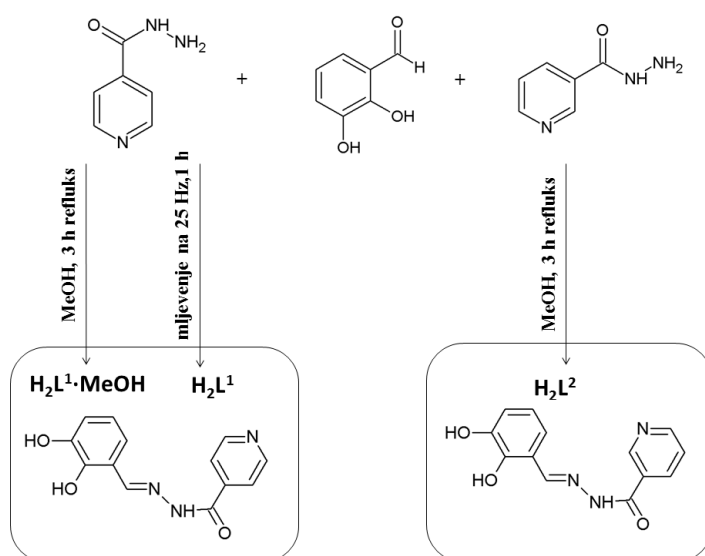
Slika 1. Reakcijski putevi sinteze hidrazonskih liganda

Difraktogram praha liganda dobivenog mehanokemijskom sintezom nije odgovarao difraktogramu produkta dobivenog otopinskom sintezom, te je produkt dobiven mehanokemijski potvrđen usporedbom s generiranim difraktogramom praha liganda poznatog iz CCDC baze. Iz kristalne strukture liganda dobivenog u otopini, vidljivo je kako ona sadržava molekulu metanola, tj. solvat je.

U slijedećem koraku provedena je reakcija između [MoO$_2$(acac)$_2$] i odgovarajućeg hidrazona (u molarnom omjeru 1:1), u acetonitrilu i metanolu. Dobivena su četiri različita kompleksa, dva polimerna iz acetonitrila, [MoO$_2$(L^1)]$_n$·MeCN, **1·MeCN** i [MoO$_2$(L^2)]$_n$, **2** te dva monomerna [MoO$_2$(L^{1,2})(MeOH)], **1a** i **2a** iz metanolne otopine. Polinuklearni kompleks **1·MeCN** je grijan na 120 °C tijekom dva sata te je dobiven kompleks **1**. Mononuklearni kompleksi su također dobiveni i mehanokemijskom sintezom potpomognuto kapljevinom nakon dva sata mljevenja na 25 Hz. Osim toga, moguća je transformacija polinuklearnih kompleksa u odgovarajuće mononuklearne refluksiranjem u metanolu tijekom 2 sata (i obratno) (Slika 2) .
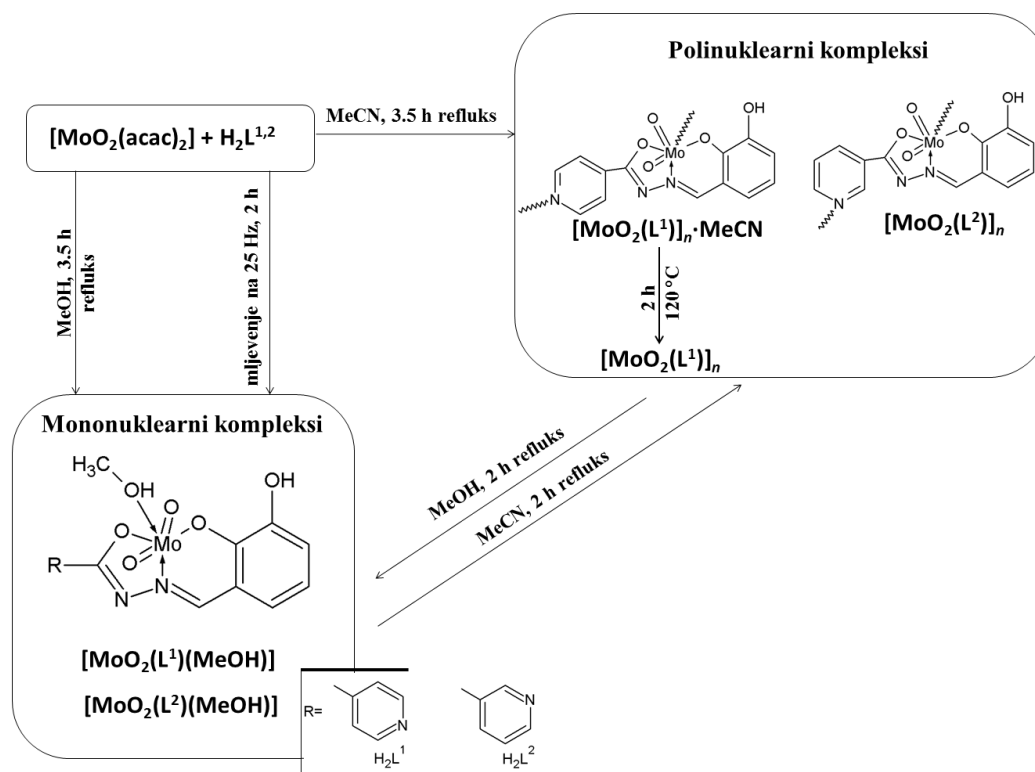
Slika 2. Reakcijski putevi sinteze kompleksa

Polinuklearne i mononuklearne komplekse moguće je razlikovati infracrvenom spektroskopijom. U spektrima mononuklearnih kompleksa uočene su dvije apsorpcijske vrpce (oko 930 i 880 cm^{-1}) istezanja MoO$_2$$^{2+}$ jezgre, te dvije vrpce koje pripadaju C–O i O–H istezanjima koordinarne molekule metanola. Na temelju vibracijske vrpce oko 910 cm^{-1} karakteristične za v_{asim}(O=Mo–N) zaključeno je kako se polimerizacija u kompleksima **1·MeCN**, **1** i **2** odvila preko dušika izonikotinskog ili nikotinskog prstena susjedne molekule. Prema podatcima termogravimetrijske analize, teorijski udjeli molibdena i molekula otapala u kompleksima su u skladu s eksperimentalno dobivenima. Također, eksperimentalni rezulati elementne analize su u skladu s teorijskim udjelima. Polinuklearni kompleksi su dodatno okarakterizirani NMR spektroskopijom, dok je mononuklearnom kompleksu **1a** određena molekulska i kristalna struktura difrakcijom rentgenskog zračenja na monokristalnom uzorku.

Pripravljeni kompleksi ispitani su kao katalizatori u reakcijama oksidacije sekundarnih alkohola, carveola i cikloheksanola. Cilj je bio odrediti utjecaj (a) supstituenta na ligandu (b) tip kompleksa (mononukelarni, polinuklearani) i (c) oksidansa (H$_2$O$_2$ i TBHP (u vodenoj otopini ili otopina u dekanu) na katalizu. Molarni omjer katalizatora, alkohola i oksidansa iznosio je: 1 : 400 : 800. Otopina alkohola, katalizatora i oksidansa u acetonitrilu je zagrijavana na 80 °C tijekom 5 sati. U određenim vremenskim intervalima su iz reakcijske smjese uzimani alikvoti, razrijeđeni s acetonitrilom te analizirani plinskom kromatografijom. Konverzija alkohola i formacija produkata su izračunati prema unutarnjem standardu, acetofenonu.

Oksidacijom smjese *cis-* i *trans-* karveola u prisutnosti H$_2$O$_2$ postignute su dobre vrijednosti konverzije karveola (84–87 %), dok su one u slučaju TBHP u vodenoj otopini bile nešto niže (56–66 %). Velika razlika u utjecaju ova dva oksidansa na katalizu vidljiv je u postignutim selektivnostima prema karvonu. U slučaju H$_2$O$_2$ selektivnost je iznosila oko 42%, dok je u slučaju TBHP u vodenoj otopini postigla vrijednosti 10–19% . Razlog tome je stereoselektivnost reakcije prema *cis-*, odnosno *trans-*karveolu. Naime, oksidacijom H$_2$O$_2$ preferirani supstrat je *cis-*karveol i glavni produkt je karvon. Suprotno tome, oksidacija *trans-*karveola vodenom otopinom TBHP-a vodi k stvaranju neidentificiranog produkta u velikoj količini. Općenito se niska selektivnost prema karvonu može objasniti time što karveol i karvon imaju dvije dvostruke veze te mogu nastati dva potencijalna epoksida, što u konačnici vodi k stvaranju nusprodukata. Otopina TBHP-a u dekanu ispitana je samo u jednoj

katalitičkoj reakciji jer je unatoč visokoj konverziji (99 %), selektivnost prema karvonu bila vrlo niska (4 %).

Pri spomenutim molarnim omjerima ispitana su samo dva katalizatora u reakcijama oksidacije cikloheksanola čime je postignuto 11–13 % konverzije u prisutnosti H_2O_2 i dobra selektivnost prema cikloheksanonu (59–64 %). Oksidacijom cikloheksanola u prisutnosti otopine TBHP-a u dekanu postignuta je najveća konverzija (28 %). Povećan je udio katalizatora, te je novi molarni omjer katalizatora, alkohola i H_2O_2 iznosio: 1 : 100 : 300. Pri ovim uvjetima, postignuto je 21 % konverzije cikloheksanola i 66 % selektivnosti prema cikloheksanonu za jedan od kompleksa.

Budući da su kompleksi u spomentim reakcijama dali vrlo slične rezultate, zaključeno je kako supstituent i tip kompleksa nemaju značajni utjecaj na katalizu. U slučaju karveola, oksidans ima značajan utjecaj na stereoselektivnost reakcije, a time i na selektivnost prema karvonu, zbog čega se H_2O_2 pokazao boljim oksidansom. Oksidacija cikloheksanola se odvija sporo s dobrom selektivnošću prema cikloheksanonu zbog čega bi trebalo produljiti vrijeme reakcije i dodatno ispitati utjecaj oksidansa.

§ 1. INTRODUCTION

Molybdenum(VI) complexes with hydrazones became an interesting area of research because of their catalytic activity. Hydrazones can act as tridentate ligands and coordinate the molybdenum atom through ONO donor set. Depending on the reaction conditions, dioxomolybdenum(VI) complexes can form different supramolecular assemblies, monomers and polymers that can be already distinguished by IR.

Catalytic oxidation of alcohols to corresponding carbonyl compounds, aldehydes and ketones is of great importance in the cosmetics, perfumery, insecticides, biofuels and pharmaceutical industries. Oxidation of carveol and cyclohexanol will be discussed in this research. Expected product in oxidation of carveol is 4R-(−)-carvone which gives characteristic odor to sweet spearmint. Cyclohexanol and its corresponding ketone, cyclohexanone are used as starting materials in the synthesis of caprolactam and adipic acid, intermediates in the production of nylon 6 and nylon 66.

The aims of this diploma thesis were: a) synthesis and structural characterization of hydrazones, b) synthesis and structural characterization of dioxomolybdenum(VI) complexes with hydrazone- based ligands, c) testing of obtained complexes as catalysts for oxidation of secondary alchohols in the presence H_2O_2 and TBHP (in aqueos solution or solution in decane)

The great emphasis in this research is on the principles of green chemistry (clean sustainable synthesis with less or without solvent, low energy consumption, use of safer chemicals). In order to respect those principles, the idea was to implement mechanochemical insted of conventional synthesis wherever possible. Succesfull solid state synthesis of one of the ligands and mononuclear complexes were carried out using the LAG method. All the complexes were characterized by IR spectroscopy, elemental and thermogravimetric analysis. In addition, polynuclear complexes were characterized by NMR and mononuclear and crystal structures of the ligand H_2L^1 and its mononuclear complex $[MoO_2(L^1)MeOH]$ were determined by the X-ray diffraction. Also, since the traditional oxidation processes often involve the use of dangerous and harmful oxidants, one goal was to develop environmentally acceptable catalytic procedure that involve green ones, *e. g.* H_2O_2 and TBHP and low catalyst loading in oxidation reactions of secondary alcohols.

§ 2.   LITERATURE REVIEW

2.1.   Hydrazones

2.1.1. Hydrazones in general

Hydrazones are Schiff bases with general formula $R^1R^2C=N-N(H)-C(=O)R^3$ (Fig. 1). They can be easily synthesized by condensation of hydrazide with a carbonyl compound (aldehyde or ketone). Hydrazones show stability towards hydrolysis, high coordination capability and can form stable complexes with transition metal ions[1].

Fig. 1. General scheme of hydrazones.

In solution, hydrazones can exist as configurational isomers (in E or Z form), Fig. 2, or in tautomeric forms (=N–NH–C=O, keto form) or (=N–N=(C–OH, enol form)) that occur in equilibrium (Fig. 3).

Fig. 2. Configurational isomers of hydrazones.

Fig. 3. Tautomeric forms of hydrazones: 3a. keto, 3b. enol form.

Hydrazones can bind to a metal center in the neutral (H_2L), singly (HL^-) and doubly-deprotonated (L^{2-}) form (after deprotonation of NH or/and OH).[1]

2.1.2. Applications of hydrazones

The azomethine group (–C=N–N) is responsible for attractive properties of hydrazones: azomethine group shows imino and amino character and imine carbon has nucleophilic and electrophilic properties. [1]

The azomethine linkage is also responsible for the antimicrobial activity and the reason why some of their primary uses are as starting materials in the synthesis of important antibacterial, antiallergic and antitumor substances. Hydrazones based ligand derived from 2,3-dihydroxybenzaldehyde and its molybdenum(II) complex showed antibacterial activity against *Pseudomonas aeruginous.* [2] It is interesting to mention that 2,3-dyhidroxybenzaldehyde exhibited antimicrobial activity against bovine mastitis *Staphylococcus aureus* strains. [3] Nicotinic hydrazide, isonicotinic hydrazide and corresponding hydrazones derived from pyridinic aldehydes have antitubercular activity. Transition metals complexes with hydrazones exhibited antibacterial and antifungal activities.[4, 5] Application of transition metal complexes derived from hydrazones is beyond their potential as therapeutic agents. Due to the structural flexibility, as well as magnetic and electrical properties, they are used in industry as catalysts, material science, nanotechnology, and electrochemistry. For example, indole-3-carboxaldehyde based hydrazone complexes with Mn(II), Co(II), Ni(II) and Zn(II) show corrosion inhibition properties.[6]

2.2. Molybdenum

Molybdenum is the only member of the second transition series with known biological functions.[7] It can be found in a wide range of metalloenzymes in plants, animals and microorganisms due to the solubility in water and a large number of available oxidation states. Molybdenum is a trace element in biological systems and molybdenum-containing enzymes are responsible for metabolism of carbon, nitrogen and sulfur. These enzymes can have multinuclear (nitrogenases) and mononuclear (oxidases, hydroxylases, reductases) active sites.[7, 8]

2.2.1. Dioxomolybdenum(VI) complexes with hydrazones

Dioxomolybdenum(VI) complexes are usually prepared from cis-$\{MoO_2\}^{2+}$ starting compound ($e.g.$ $[MoO_2(acac)_2]$, $[MoO_2X_2]$, $[MoO_2X_2(L)_2]$ (X= halide, L= H_2O, DMSO, OPPh$_3$)) in the reaction with an appropriate ligand. Most commonly, hydrazones can act as tridentate ligands and coordinate the molybdenum atom through ONO donor set. Depending on the reaction conditions (starting compunds, temperature, solvent), dioxomolybdenum(VI) complexes can form different supramolecular assemblies that can be already distinguished by IR. The IR spectra of mononuclear complexes, $[MoO_2(L)(D)]$ (L = tridentate ligand, D = donor molecule, $e.g.$ methanol) have two vibration bands in the region 880–950 cm^{-1} characteristic for $v(MoO_2)$ vibrations. A band at around 1050 cm^{-1} is assigned to the C–O stretching vibration of the coordinated methanol molecule. In polynuclear complexes, $[MoO_2(L)]_n$ terminal oxygen atom or nitrogen atom from the neighboring hydrazone ligand can coordinate a metal center. If polymerization occurs through nitrogen, a band at around 910 cm^{-1} assigned to v_{asym}(O=Mo–N) is present. [9, 10] However, polymerisation is mostly achieved through terminal oxygen atom and in IR spectra can be seen broad band characteristic for an intermolecular Mo=O···Mo interaction (vibration band at around 850 cm^{-1} for dinuclear or 800 cm^{-1} for polynuclear complex).[11, 12] Lastly, in dioxomolybdenum(VI) complexes with pyridoxal hydrazones polymerization can occur via an oxygen atom from hydroxymethyl group. In this case two intense bands at ca. 950 cm^{-1} and 900 cm^{-1} are present in the spectra.[13]

More detailed reaction conditions of synthesis of molybdenum(VI) complexes with hydrazones, their structures and structural transformations are presented below.

In the first example, mononuclear complexes were synthesized by using MoO_2Cl_2 and the corresponding isonicotinoylhydrazone ligand in dry methanol.[9] Three types of ligands, H_2L^R were used: salicylaldehyde isonicotinoylhydrazone (H_2L^{SIH}), 2-hydroxy-naphtaldehyde isonicotinoylhydrazone (H_2L^{NIH}), or p-(N,N´-diethylamino)salicylaldehyde isonicotinoylhydrazone ($H_2L^{Et2NSIH}$).

In all mononuclear complexes, $[MoO_2(HL^R)(MeOH)]Cl$ the *cis*-$\{MoO_2\}^{2+}$ core is coordinated by the singly-deprotonated ligand *via* ONO donor atoms and by a solvent molecule, MeOH. After exposure of complexes to water vapor the coordination sphere around the molybdenum atom was changed and completed by coordination of a water molecule.

Molecular structures of mononuclear complexes with salicylaldehyde isonicotinoylhydrazone, $[MoO_2(HL^{SIH})(MeOH)]Cl$ and with 2-hydroxy-naphtaldehyde isonicotinoylhydrazone, $[MoO_2(HL^{NIH})(H_2O)]Cl$ are shown in Fig. 4 and 5, respectively.

Fig. 4. Molecular structure of $[MoO_2(HL^{SIH})(MeOH)]Cl$ complex.[9]

Fig. 5. Molecular structure of $[MoO_2(HL^{NIH})(H_2O)]Cl$ complex.[9]

Mononuclear complex [MoO$_2$(HL^{Et2NSIH})(MeOH)]Cl can be deprotonated and transformed into polynuclear complex [MoO$_2$(L^{Et2NSIH})]$_n$ by mechanochemical or solution-based methods (by using Et$_3$N as a base) or employing photoassisted deprotonation (without using a base). Van der Waals interactions connect chains into polymeric zig-zag structure, while polymerisation occurred through nitrogen atom. (Fig. 6).

Fig. 6. Two polymeric chains in [MoO$_2$(L^{Et2NSIH})]$_n$.[9]

Most recently[10], molybdenum complexes with the various nicotinoyl-based ligands were reported. Here are presented mononuclear and polynuclear complexes with salicylaldehyde nicotinoylhydrazone, H$_2$L^H.

A series of reactions between [MoO$_2$Cl$_2$] or [MoO$_2$(acac)$_2$] and a ligand, H$_2$L^H in methanol or ethanol yielded coordination polymer or monomers depending on the reaction conditions (temperature, solvent, cis-{MoO$_2$}$^{2+}$ starting compound).

Monomer, [MoO$_2$(L^H)(MeOH)] (Fig. 7) was obtained from the reaction between [MoO$_2$Cl$_2$] or [MoO$_2$(acac)$_2$] in methanol at room temperature. Different monomer, [MoO$_2$(HL^H)(MeOH]Cl (Fig. 8) can be synthesized from [MoO$_2$Cl$_2$] in methanol at −5 °C.

Fig. 7. Molecular strucuture of a monomer, [MoO$_2$(L^H)(MeOH)] obtained from [MoO$_2$Cl$_2$] or [MoO$_2$(acac)$_2$] and salicylaldehyde nicotinoylhydrazone, H$_2$L^H (methanol, room temperature).[10]

Fig. 8. Molecular strucuture of a monomer, [MoO$_2$(HL^H)(MeOH)]Cl obtained from [MoO$_2$Cl$_2$] and salicylaldehyde nicotinoylhydrazone, H$_2$L^H (methanol, –5 °C).[10]

Coordination polymer, [MoO$_2$(L^H)]$_n$ (Fig.9) can be obtained by direct synthesis from [MoO$_2$Cl$_2$] (in methanol) or [MoO$_2$(acac)$_2$] (in ethanol) at 110 °C, or by transformation of mononuclear complex, [MoO$_2$(L^H)(MeOH)] in thermally induced solid-state reaction. Deprotonation of nitrogen resulted in its coordination to the Mo atom from the neighboring molecule.

Fig. 9. Molecular structure of a coordination polymer, $[MoO_2(L^H)]_n$ obtained from $[MoO_2Cl_2]$
or $[MoO_2(acac)_2]$ and salicylaldehyde nicotinoylhydrazone, H_2L^H
(methanol, 110 °C) or from monomeric complex, $[MoO_2(L^H)(MeOH)]$ in thermally induced
solid-state reaction.[10]

In all complexes, the Mo atom displays a slightly distorted octahedral coordination involving nitrogen and two oxygen atoms from *cis*-$\{MoO_2\}^{2+}$ unit. The sixth coordination place is occupied with the oxygen atom from a methanol molecule or nitrogen atom from the pyridine moiety of the neighboring molecule.

2.3.   Mechanochemical synthesis

When talking about green chemistry one of the first things that come to our mind is clean, sustainable and environmentally friendly synthesis with low energy consumption. Although classical solution-based synthesis is irreplaceable in certain synthetic processes, its use is attempted to be reduced due to a large amount of used solvent. Also, the drawback is the long duration of the synthesis which results in the formation of undesired by-products and high energy consumption. The idea is to replace solution-based synthesis where is possible with a synthesis that employs a minimal amount of solvent or, in the best case, is solvent-free. If the synthesis can be carried out in the solid phase, one possibility is mechanochemical synthesis.[14] According to IUPAC, mechanochemical process is: ″a chemical reaction that is induced by direct absorption of mechanical energy″.[15]

Mechanochemical reactions can be carried out using different methods, for example, mortar and pestle or ball mill. Neat grinding (NG) considers the reaction conducted without the addition of liquid. When a very small amount of a liquid is added to the reaction mixture,

it is called liquid assisted grinding (LAG). The purpose of added liquid is to assist molecular diffusion.

Monitoring of the reaction in the solid-state offers possibility to understand reaction mechanisms and gives insight into the whole process. For real-time *in-situ* reaction monitoring, Raman spectroscopic technique with translucent milling chamber can be employed. If reaction is air, moisture or CO_2 sensitive, then *in situ* analysis is necessary. In case of *ex-situ* analysis, grinding is stopped and a sample of reaction mixture obtained after a particular reaction time can be analyzed by using several methods (PXRD, DSC, IR-spectroscopy). [14, 16]

2.4. Catalytic oxidation of secondary alcohols

2.4.1. Introduction to catalysis

Catalyst is material added in the reaction mixture in a small quantity that increases the rate of the studied chemical reaction. Catalyst accelerates a chemical reaction by forming bonds with reactants and letting them react with each other without affecting the position of the equilibrium and thermodynamics of the reaction. At the end of the reaction cycle, products desorb from the catalyst. In an ideal case, the catalyst is recovered in its original form and ready for another reaction cycle. Unfortunately, catalyst's lifetime is limited. Structural changes during chemical reactions can lead to the deactivation of the catalyst, so catalyst must be reactivated or replaced. [17]

In general, catalysts can be classified as: i) molecular and ii) supported ones. Molecular catalysts are often coordination complexes that are transformed into their active form during the reaction.[18-20] Supported catalysts are composed of an active phase scattered on the carrier. Components (active species, promoters and supports), shape, size pore volume, surface area, catalyst leaching, regeneration and toxicity as well as an acceptable price, should be considered when designing such catalysts. The most commonly used carriers are SiO_2, Al_2O_3 and active coal, while preparation methods are impregnation, ion-exchange, adsorption and deposition-precipitation.[21]

Based on that, two types of catalysis can be distinguished. Homogeneous catalysis involves a system in which catalysts, reactants, and products are in the same phase, implying the use of molecular catalysts. In cases in which catalysts, reactants, and products occur in different phases, the process is considered as heterogeneous catalysis. Mainly, the catalyst is solid and the reactants are liquids or gases.

Green catalysis, as a subcategory of green chemistry, has a goal to develop catalysts with higher activity and selectivity. The catalyst should be easily recovered and durable. Briefly, the idea is to design a cleaner and greener chemical process and produce purer products.[17]

Generally, reaction where **R** is reactant, **P** is a product and **cat** is catalyst can be described as followed:

$$R \xrightarrow{cat} P$$

Conversion (CON), selectivity (S), turnover number (TON), turnover frequency (TOF) and mass balance are parameters that describe the efficiency of the catalytic process. Conversion, selectivity and mass balance can be expressed in percentage.

- Conversion (CON) of reactant R is the ratio between the amount of transformed reactant R, $n_{R transformed}$ up to the defined reaction time, t, and the amount of reactant added at the beginning of the reaction, $n_{R(0)}$ (equation 1).

$$CON = \frac{n_{R\,transformed}}{n_{R(0)}} = \frac{n_{R(0)} - n_{R(t)}}{n_{R(0)}} \quad (1)$$

- Selectivity (S) towards the desired product is defined as the ratio between product P formed, $n_{P(t)}$ and the reactant R transformed, $n_{R transformed}$ up to the defined reaction time, t (equation 2).

$$S = \frac{n_{P(t)}}{n_{R\,transformed}} = \frac{n_{P(t)}}{n_{R(0)} - n_{R(t)}} \quad (2)$$

- Turnover number (TON) is mathematically expressed as the amount of product P, $n_{P(t)}$ formed up to defined reaction time, t divided with the amount of catalyst, n_{cat}. TON gives the number of reactant molecules that one molecule of the catalyst can convert (equation 3).

$$TON = \frac{n_{R\,transformed}}{n_{cat}} = \frac{n_{R(0)} - n_{R(t)}}{n_{cat}} \quad (3)$$

- Turnover frequency (TOF) is mathematically defined as the amount of transformed reactant, $n_{Rtransformed\ in\ \Delta t}$ in time interval (between t_x and t_{x+1}) divided with the amount of catalyst, n_{cat} and time interval, Δt. TOF gives number of transformed reactant molecules per time unit (equation 4).

$$\text{TOF} = \frac{n_{R\ transforemd\ in\ \Delta t}}{n_{cat}} \times \frac{1}{\Delta t} = \frac{n_{R(t_x)} - n_{R(t_{x+1})}}{n_{cat}} \times \frac{1}{t_{x+1} - t_x} \quad (4)$$

- Mass balance is described as the number of reactants, $n_{R(t)}$ and products, $n_{P(t)}$ at the defined time, t divided with the amount of reactant added at the beginning of the reaction, $n_{R(0)}$ (equation 5).

$$\text{Mass balance} = \frac{n_{R(t)} + n_{P(t)}}{n_{R(0)}} \quad (5)$$

2.4.2. Oxidation of secondary alcohols

Catalytic oxidation of alcohols to corresponding carbonyl compounds, aldehydes and ketones is of great importance in the cosmetics, perfumery, insecticides, biofuels and pharmaceutical industries.

Since the traditional oxidation processes often involve the use of dangerous and harmful oxidants, such as $KMnO_4$, CrO_3 and halogenated solvents, there is a definite need for developing more environmentally and economically acceptable catalytic procedures that involve green oxidants. An example of an oxidant with an environmentally friendly nature is hydrogen peroxide, H_2O_2. *Tert*-butyl hydroperoxide (TBHP) is also an option because its solubility and stability in organic solvents, providing attractive properties.[22] Further, the by-product of the reaction, *tert*-butanol (*t*BuOH) can be easily separated by destilation, recycled into methyl *tert*-butyl ether (MTBE) and reused as a gasoline additive.[23]

The subject of this study is the oxidation of secondary alcohols, carveol and cyclohexanol to the corresponding ketones, carvone and cyclohexanone (Fig. 10).
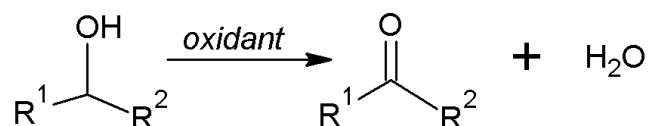
Fig. 10. General scheme of the oxidation of secondary alcohol to the corresponding ketone.

2.4.3. Carveol and carvone

Carveol is usually used as a mixture of *cis-* and *trans-* isomers. Since the *trans-* carveol is an expensive ingredient of Valencia orange essential oil used in perfume bases and food flavors, interest in selective synthesis is on the rise.[24] The successful selective synthesis was carried out from α-pinene oxide catalyzed by zeolite catalyst.[25]

The corresponding ketone, expected in this reaction, 4*R*-(−)-carvone, gives characteristic odor to sweet spearmint (Fig. 11). Carvone also plays a big role in the production of pharmaceuticals, fragrances and flavors. It can be extracted from essential oils of spearmint but the great demand has stimulated the development of new chemical pathways for the production of carvone. The catalytic oxidation of limonene obtained from the waste orange peels to the limonene oxides, carvone and carveol is perfect example of sustainable development.[26, 27]
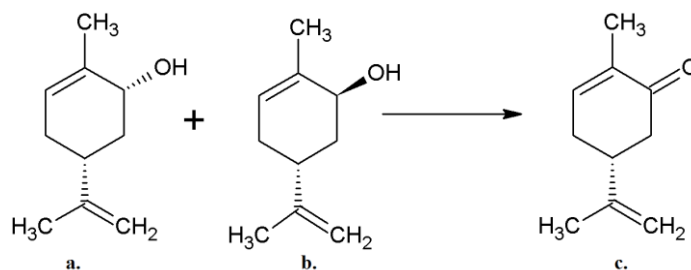
Fig. 11. Oxidation of (−)-*cis-* (a.) and (−)-*trans-* (b.) carveol to the 4*R*-(−)-carvone (c.).

Recently catalytic oxidation of carveol with hydrogen peroxide in the presence of 0.3 % of catalyst, $Mn_4(PW_9)_2$, $Co_4(PW_9)_2$ and $Fe_4(PW_9)_2$ was reported. The results showed a very good conversion, around 99 %. However, selectivity towards carvone was between 45-51 %, carveol 1,2-epoxide was yielded in similar amount and carveol 8,9-epoxide was also present but in small quantity (Fig. 12).[28]
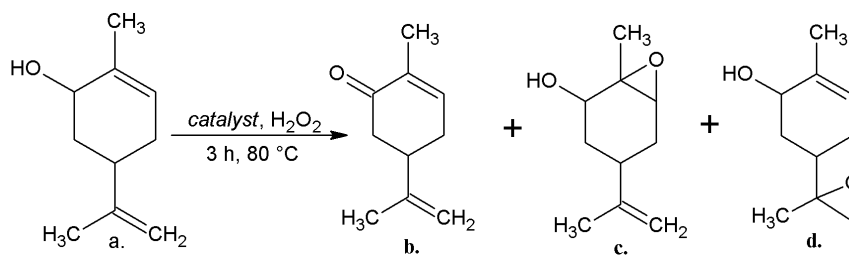
Fig. 12. Oxidation of carveol by hydrogen peroxide catalyzed by $M_4(PW_9)_2$ heteropolyanions (M=Co(II), Mn(II), Fe(II)): a. carveol, b. carvone, c. carveol 1,2-epoxide, d. carveol 8,9-epoxide.[28]

Slightly less selectivity towards carvone (40 %) with 75 % conversion of carveol were achieved with TBHP over the phthalocyanine complex $FePcCl_{16}$ immobilized on the mesoporous silica SBA-15.[29]

These studies confirm the assumption that high selectivity in the carveol oxidation reaction is quite difficult to achieve. Two double bonds can be transformed during the reaction and epoxidation can occur.

2.4.4. Cyclohexanol and cyclohexanone

Cyclohexanol and cyclohexanone are colorless, moderately toxic, not corrosive to iron or steel and soluble in most organic solvents. The majority of these compounds and their mixtures are used as starting material in the synthesis of caprolactam and adipic acid, intermediates in the production of nylon 6 and nylon 66.[30] Adipic acid is utilized in the production of plastics, textiles, lubricants, and as a supplement in the food and cosmetic goods. Since the traditional production of adipic acid brings the safety and environmental impact in question, scientific research is directed at adipic acid being catalytically produced from cyclohexanone with molecular oxygen.[31] (Fig. 13) or hydrogen peroxide[32] as an oxidizing agent.
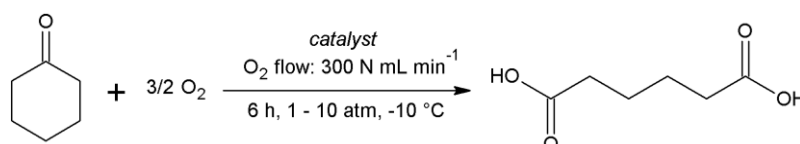
Fig. 13. Adipic acid synthesis from cyclohexanone oxidation with an oxygen and Keggin-type P/Mo/V polyoxometalates used as homogeneous catalysts and carried out in a semi-continuous stirred autoclave reactor.[31]

Cyclohexanone can also be employed as thinner or solvent for synthetic resins and polymers or as a starting substance in the manufacture of insecticides and herbicides.[30] Multiple application and high demand bring new insights when it comes to the catalytic dehydrogenation of cyclohexanol to cyclohexanone (Fig. 14).
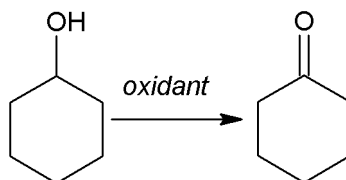
Fig. 14. Oxidation of cyclohexanol to cyclohexanone.

The oxidation in water catalyzed by supported phosphotungstic acid (PTA) on silica-coated $MgAl_2O_4$ nanoparticles with hydrogen peroxide is impressive since catalyst showed recoverable properties.[33] Copper oxide dispersed on mesoporous material with less than 10 % Cu content showed the most effective catalytic activity in a continuous flow gas phase reactor.[34] The reaction of cyclohexanol gave the targeted product in 82-97 % in presence of 1 % of ruthenium pyridine-imine based complexes with N-methylmorpholine-N-oxide (NMO). NMO, stable nitroxyl radical, is a known oxidant for selective oxidation of alcohols under mild conditions.[35]

Despite high results, selective conversion of cyclohexanol to cyclohexanone can be challenging. Limiting factors can be reversibility of the reaction, the steric effect of cyclohexyl group and competing reactions (aromatization to phenol, dehydration to cyclohexene and condensation of cyclohexanone to cyclohexenyl cyclohexanone).[34]

2.4.5. Molybdenum complexes as catalysts in oxidation reactions of secondary alcohols
To the best of our knowledge, molybdenum complex with hydrazones have not been described as catalysts in oxidation of carveol and cyclohexanol. However, examples of their catalytic activity in oxidation of other secondary alcohols are presented below.

In the first case[36], dioxomolybdenum(VI) complexes with ONO donor ligands obtained by the condensation of 2,6-diformyl-4-methylphenol and hydrazides (benzoyl, isonicotinoyl and nycotinoyl hydrazide) and hydrogen peroxide served as successful catalytic system for oxidation of 1-phenyl ethanol, propan-2-ol and butan-2-ol (Fig. 15). Benzoylhydrazide based complex and 1-phenyl ethanol were selected as representatives for optimization reaction

conditions. 5 mmol of 1-phenyl ethanol, 15 mmol of H_2O_2 and 3.5×10^{-3} mmol of catalyst (0.07 %) in 5 mL of CH_3CN were used. 91 % of alcohol was transformed into the desired product, Fig. 15, (after 20 h and at the reaction temperature of 80 °C). Oxidations of two other alcohols, under the optimized reaction conditions, provided good catalytic results.
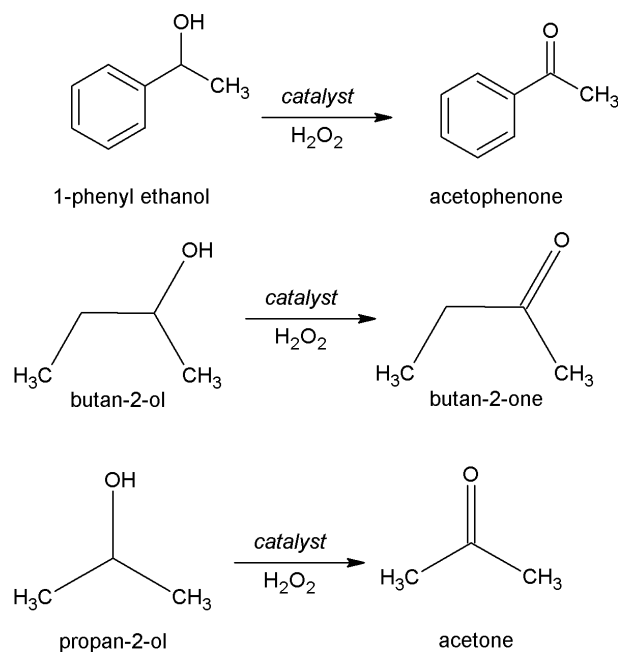
Fig. 15. Oxidation of secondary alcohols to the corresponding ketones.[36,37]

Another catalytic testing employed dioxomolibdenum(VI) complexes with ligands derived from 4-benzoyl-3-methyl-1-phenyl-2-pyrazoline-5-one and isonicotinoyl, benzoyl, nicotinoyl or furoyl hydrazide, as catalysts, while the same substrates, as in the first case, were used. Catalytic conditions in which were used 10 mmol of 1-phenyl ethanol, 30 mmol of H_2O_2 and 1.8×10^{-3} mmol of catalyst (0.018 %) in 10 mL of CH_3CN proved to be the most efficient (after 20 h and under 80 °C reaction temperature).[37]

§ 3.   EXPERIMENTAL SECTION

Reagents and solvents used for the synthesis were commercially available and employed without further purification.

Attenuated Total Reflection (ATR) Infrared spectra (IR) were recorded with a Perkin–Elmer 502 spectrophotometer in the region of $4000-400 \ cm^{-1}$.

Thermogravimetric (TG) analysis were carried out with a Mettler-Toledo TGA/SDTA851 thermobalance using aluminum crucibles, under the oxygen atmosphere and within the temperature range from 25 to 600 °C with a heating rate of 10 °C min^{-1} and analyzed by the Mettler STAR^e 15.01. Software.

Differential Scanning Calorimetry (DSC) measurements were performed using a Mettler–Toledo DSC823^e calorimeter and analyzed by the Mettler STAR^e 9.01. Software.

The samples for powder X-ray diffraction were recorded on a Si sample holder. Measurements were carried out with a Panalytical X'Change powder diffractometer in the Bragg–Brentano geometry using Cu-$K\alpha$ radiation. Patterns were collected in the range of $2\theta =$ 5–50° with a step size of 0.020 ° and at 1.0 s per step. In the case of *ex-situ* reaction monitoring, patterns were collected in the range of $2\theta = 4-50°$ with the step size of 0.020 ° and at 0.40 s per step The data were collected and visualized using the X'Pert programs Suite.

Molecular and crystal structures were determined by the single-crystal X-ray diffraction at the Division of General and Inorganic Chemistry. The analysis was done by Ivica Đilović, Assistant Professor and Edi Topić, Ph.D. Student.

For complexes identification, 1D (^{1}H, ^{13}C-DEPTq) and 2D (COSY, HSQC, HMBC) solution NMR spectra were recorded on Bruker Avance III HD 400 MHz/54 mm Ascend spectrometer equipped with a 5 mm PA BBI 1H/D-BB Z-GRAD probe head. All measurements were performed at 298 K using standard Bruker pulse programs. DMSO-d_6 was used as solvent and TMS as an internal standard for proton and carbon chemical shifts.

Chromatograms were obtained using Agilent 7820A chromatograph with FID detector and DB-WAX capillary column (30 m x 0.32 mm x 0.5 μm). The GC analysis were conducted as follows: 70–240 °C with a 20 °C min^{-1} ramp and 2 mL min^{-1} flow rate, while in case of cyclohexanol reaction mixtures with TBHP conditions were: 50–240 °C with a 5 °C min^{-1} ramp and 2 mL min^{-1} flow rate. GC parameters were quantified with commercially available

samples of the substrates and expected products. Conversion of secondary alcohols and formation of corresponding ketones were calculated from calibration curves relative to acetophenone as an internal standard.

Liquid assisted grinding (LAG) experiments were performed using a Retsch MM200 ball mill at 25 Hz .

3.1. Preparation of the starting compounds

3.1.1. Dioxobis(2,4-pentanedionato)molybdenum(VI), [MoO₂(acac)₂]

10 mL of aqueous solution of ammonium heptamolybdate tetrahydrate $(NH_4)_6Mo_7O_{24}\cdot4H_2O$, (3 g, 0.04 mmol) was prepared and 4 mL (2.4 mmol) of acetylacetone $C_5H_8O_2$ was added. A pH value of the solution was adjusted to 3.5 with the addition of HNO_3 (w=10 %) and stirred for one hour in the dark. A yellow product was separated by filtration after 2 hours and rinsed with water and ethanol.

3.1.2. Hydrazone based ligands

Solution-based synthesis:

2, 3-dihydroxybenzaldehyde (0.1500 g, 1 mmol) was dissolved in 50 mL of hot methanol and corresponding hydrazide (0.1489 g, 1 mmol) was added. The reaction mixture was refluxed for 3 hours. In both cases, the yellow crystalline product was formed after few days and separated by filtration.

a) 2, 3-dihydroxybenzaldehyde isonicotinoylhydrazone, H₂L¹·MeOH

Yield 0.1175 g (45 %).

IR: ($\tilde{v}_{max}$ / cm⁻¹): 1679 (C=O), 1619 (N=C), 1289, 1270 (C–O$_{phenyl}$), 1151 (N–N).

DSC: (after prolonges standing at the room temperature) $\Delta_{fus} H = 46$ kJ mol⁻¹, $T_m = 258$ °C.

(see Appendix, Fig. D1 for IR and Fig. D11 for DSC)

b) 2, 3-dihydroxybenzaldehyde nicotinoylhydrazone, H₂L²

Yield 0.1195 g (47 %).

IR: ($\tilde{v}_{max}$ / cm⁻¹): 1667 (C=O), 1609 (N=C), 1284, 1263 (C–O$_{phenyl}$), 1152 (N–N).

DSC: $\Delta_{fus} H = 40$ kJ mol⁻¹, $T_m = 252$ °C.

(see Appendix, Fig. D3 for IR and Fig. D12 for DSC)

Mechanochemical synthesis:

*2, 3-dihydroxybenzaldehyde isonicotinoylhydrazone, **H₂L¹***

0.1500 g (1 mmol) of 2, 3-dihydroxybenzaldehyde and 0.1489 (1 mmol) of isonicotinic hydrazide were placed in a Teflon jar. 50 µL of methanol was added to the mixture. The mixture was milled at 25 Hz for 60 min.

Yield: 99 %.

IR: ($\tilde{v}_{max}$ / cm^{-1}): 1673 (C=O), 1607 (N=C), 1291, 1267 (C–O$_{phenyl}$), 1153 (N–N).

(see Appendix, and Fig. D2 for IR)

3.2.   Synthesis of molybdenum (VI) complexes

3.2.1. The polynuclear complexes

0.0784 g (3.06 × 10^{-4} mol) of the corresponding ligand, **H₂L¹** or **H₂L²**, was dissolved in 50 mL of hot acetonitrile and 0.1 g (3.06 × 10^{-4} mol) of [MoO₂(acac)₂] was added. The orange reaction mixture was refluxed for 3.5 hours. In both cases, the solution was left at the room temperature to cool down and orange powder was separated by filtration.

*a) [MoO₂(L¹)]ₙ·MeCN (**1·MeCN**)*

Yield 0.0875 g (75 %).

Anal. Calcd. mass fractions of elements, *w* / %, for C$_{15}$H$_{12}$MoN$_4$O$_5$ (*M*r = 424.212) are: C 42.27, H 2.85, N 13.21; found: C 41.35, H 2.11, N, 13.00.

IR: ($\tilde{v}_{max}$ / cm^{-1}): 1602 (C=N), 1570 (C–O$_{phenolic}$), 1349 (C–O$_{hydrazone}$), 937 (Mo=O), 908 (O=Mo–N).

TG: CH₃CN, 9.37 % (Calcd. 9.67 %); MoO₃, 35.01 % (Calcd. 33.93 %).

(see Appendix, Fig. D4 for IR and Fig. D18 for TG)

*b) [MoO₂(L¹)]ₙ (**1**)*

[MoO₂(L¹)]ₙ was obtained after 2 hours of heating [MoO₂(L¹)]ₙ·MeCN at 120 °C.

Anal. Calcd. mass fractions of elements, *w* / %, for C$_{13}$H$_9$MoN$_3$O$_5$ (*M*r = 383.168) are: C 40.75, H 2.37, N 10.97; found: C 39.70, H 2.21, N 10.11.

IR: ($\tilde{v}_{max}$ / cm^{-1}): 1601 (C=N), 1570 (C–O$_{phenolic}$), 1350 (C–O$_{hydrazone}$), 937 (Mo=O), 910 (O=Mo–N).

TG: MoO₃, 39.74 % (Calcd. 37.57 %).

(see Appendix, Fig. D5 for IR, Fig. D19 for TG and Table. D1 for NMR)

c) $[MoO_2(L^2)]_n$ (**2**)

Yield 0.0877 g (75 %).

Anal. Calcd. mass fractions of elements, w / %, for $C_{13}H_9MoN_3O_5$ (*M*r = 383.168) are: C 40.75, H 2.37, N 10.97; found: C 39.12, H 2.01, N 9.87.

IR: ($\tilde{v}_{max}$ / cm^{-1}): 1612 (C=N), 1571 (C–O$_{phenolic}$), 1342 (C–O$_{hydrazone}$), 937 (Mo=O), 910 (O=Mo–N).

TG: MoO$_3$, 37.50 % (Calcd. 37.57%).

(see Appendix, Fig. D8 for IR, Fig. D21 for TG and Table D1 for NMR)

3.2.2. The mononuclear complexes

Solution based synthesis:

0.0784 g (3.06 × 10^{-4} mol) of the corresponding ligand, **H$_2$L^1** or **H$_2$L^2**, was dissolved in 30 mL of hot methanol and 0.1 g (3.06 × 10^{-4} mol) of [MoO$_2$(acac)$_2$] was added. The orange reaction mixture was refluxed for 3.5 hours. The solution was left at the room temperature to cool down and orange crystalline product was separated by filtration.

a) $[MoO_2(L^1)(MeOH)]$ (**1a**)

Yield 0.850 g (67 %).

Anal. Calcd. mass fractions of elements, w / %, for $C_{14}H_{13}MoN_3O_6$ (*M*r = 415.209) are: C 40.50, H 3.16, N 10.12; found: C 39.8, H 3.11, N 9.70.

IR: ($\tilde{v}_{max}$ / cm^{-1}): 1599 (C=N), 1574 (C–O$_{phenolic}$), 1334 (C–O$_{hydrazone}$), 1034 (C–O$_{MeOH}$), 930, 878 (MoO$_2$).

TG: MeOH, 7.17 % (Calcd. 7.71 %); MoO$_3$, 35.50 % (Calcd. 34.67%).

(see Appendix, Fig. D6 for IR and Fig. D20 for TG)

b) $[MoO_2(L^2)(MeOH)]$ (**2a**)

Yield 0.0824 g (66 %).

 Anal. Calcd. mass fractions of elements, w / %, for $C_{14}H_{13}MoN_3O_6$ (*M*r = 415.209) are: C 40.50, H 3.16, N 10.12; found: C 39.3, H 2.98, N 9.14.

IR: ($\tilde{v}_{max}$ / cm^{-1}): 1610 (C=N), 1564 (C–O$_{phenolic}$), 1332 (C–O$_{hydrazone}$), 1019 (C–O$_{MeOH}$), 930, 876 (MoO$_2$).

TG: MeOH, 6.72 % (Calcd. 7.71 %); MoO$_3$, 36.18 % (Calcd. 34.67%).

(see Appendix, Fig. D9 for IR and Fig. D22 for TG)

Mechanochemical synthesis:

0.0784 g (3.06 × 10^{-4} mol) of the corresponding ligand, **H$_2$L^1** or **H$_2$L^2**,   0.1 g (3.06 × 10^{-4} mol) of [MoO$_2$(acac)$_2$], and 50 μL of methanol was added to the Teflon jar. The mixture was milled at 25 Hz for 120 min.

1a:

Yield: 99 %

IR: ($\tilde{v}_{max}$ / cm^{-1}): 1601 (C=N), 1575 (C–O$_{phenolic}$), 1337 (C–O$_{hydrazone}$), 1034 (C–O$_{MeOH}$), 931, 880 (MoO$_2$).

(see Appendix, Fig. D7 for IR)

2a: Yield: 99 %

IR: ($\tilde{v}_{max}$ / cm^{-1}): 1612 (C=N), 1564 (C–O$_{phenolic}$), 1339 (C–O$_{hydrazone}$), 1020 (C–O$_{MeOH}$) 933, 879 (MoO$_2$).

(see Appendix, Fig. D10 for IR)

3.3.   *Ex-situ* solid state reaction monitoring

The liquid-assisted grinding technique (LAG) in a ball mill of the starting reagents in the presence of a small amount of methanol was used and reactions were conducted at 25 Hz and at room temperature. Performing multiple runs allowed synthesis progress to be followed *ex-situ* as a function of time without disturbing reaction mixture. **H$_2$L^1** was successfully obtained in such a way; 0.1500 g (1 mmol) of 2, 3-dihydroxybenzaldehyde, 0.1489 (1 mmol) of isonicotinic hydrazide and 50 μL of methanol were used. A sample of the powder obtained after a particular reaction time (10, 20, 30, 40, 50 and 60 min) was immediately analysed by PXRD (see Appendix, Fig. D14). No purification of the sample was performed.

3.4.   General procedure for oxidation of secondary alcohols

Oxidation of secondary alcohol was carried out in a 25 mL round-bottom flask equipped with a reflux condenser. Alcohol, acetophenone (0.1 mL) and acetonitrile (2.5 mL) were stirred together. Mo(VI) (pre)catalyst was added to the mixture. The mixture was stirred and heated up to 80 °C before adding an oxidant. The obtained solution was stirred using magnetic stirrer

for 5 hours and the reaction temperature of 80° C was maintained using an oil bath. The reaction was monitored by withdrawing small aliquots of the reaction mixture at a definite time interval (0, 20, 50, 90, 150 and 300 min), mixed with acetonitrile and analyzed quantitatively by gas chromatography with acetophenone as an internal standard.

In order to find the best catalytic system, reactions were conducted under the various conditions presented below:

3.4.1. Carveol oxidation:

Reaction conditions: 10 mmol of carveol (1.6 mL), 20 mmol of oxidant (H_2O_2, w = 35 %, 1.76 mL, or **aqueous TBHP**, w = 70 %, 2.74 mL, or **TBHP in decane**, c = 5.5 mol dm^{-3}, 3.64 mL), 0.025 mmol of catalyst (0.25 %, 0.0095 g of the polymer, **1** or **2**, or 0.010 g of the monomer complex, **1a** or **2a**).

3.4.2. Cyclohexanol oxidation with H_2O_2:

Reaction conditions: 10 mmol (1.1 mL) or 5 mmol of cyclohexanol (0.54 mL), 20 mmol (w = 35 %, 1.76 mL) or 15 mmol of H_2O_2 (w = 35 %, 1.32 mL), 0.025 mmol of catalyst (0.25 %, 0.0095 g of the polymer, **1** or **2**, or 0.010 g of the monomer complex, **1a** or **2a**) or 0.05 mmol of catalyst (1 %, 0.019 g of the polymer, **1** or **2**, or 0.2 g of the monomer complex, **1a** or **2a**) and 2.5 mL of acetonitrile.

3.4.3. Cyclohexanol oxidation with TBHP:

Reaction conditions: 10 mmol of cyclohexanol (1.1 mL), 20 mmol of oxidant (aqueous TBHP, w = 70 %, 2.74 mL or TBHP in decane, c = 5.5 mol dm^{-3}, 3.64 mL), 0.025 mmol of catalyst (0.25 %, 0.0095 g of the polymer **2**, or 0.010 g of the monomer complex **2a**).

§ 4.   RESULTS AND DISCUSSION

4.4.   Hydrazone based ligands

4.4.1. Synthesis and characterization

The **H₂L^1** and **H₂L^2** ligands were prepared by condensation reaction between 2,3-dihydroxybenyaldehyde and isonicotinic or nicotinic hydrazide, respectively (Scheme 1). Reactions were conducted in absolute methanol under a reflux condenser. Obtained ligands are pale yellow crystals and moderately soluble in methanol and acetonitrile.
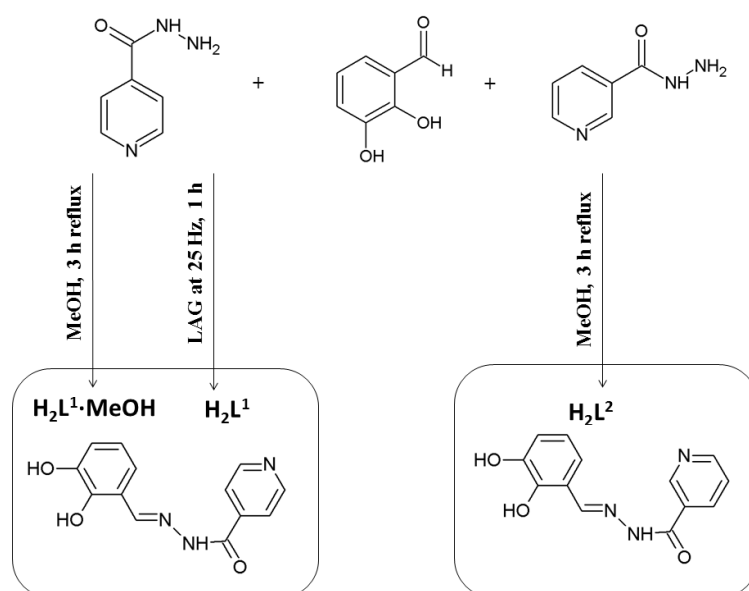
Scheme 1. Synthesis of ligands **H₂L^1** and **H₂L^2**.

Successful solid-state synthesis of isonicotinic based ligand, **H₂L^1** was carried out using the LAG method. Performing multiple runs allowed synthesis progress to be followed *ex–situ*. A sample of the powder obtained after particular reaction time was immediately analyzed by using PXRD method (no purification of the powder was performed). The formation of the desired product was confirmed by comparing powder X-ray diffraction pattern from the sample obtained after 1 h of grinding with the pattern obtained from the database[38] (Appendix, Fig. D14). **H₂L^2** ligand was not possible to synthesize in a mechanochemical way, presumably because of lower reactivity of nicotinic hydrazide.

Molecular and crystal structure of **H$_2$L^1·MeOH** is described using single-crystal X-ray crystallography (Fig. 16). It was determined that isonicotinic based hydrazone is in keto tautomeric form and contains methanol molecule in its crystal structure.
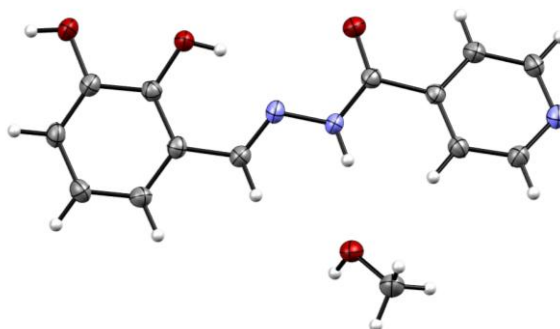

Fig. 16. Molecular structure of **H$_2$L^1·MeOH** ligand.

Different crystal structures of isonicotinic based ligands obtained from solution-based and solid-state synthesis are indicated by comparison PXRD patterns. It can be assumed that the ligand synthesized in a mechanochemical way does not contain a methanol molecule in its crystal structure, as well as the one previously described in the literature[38]. Although the crystal structure of **H$_2$L^2** has not been determined in this study, its PXRD pattern corresponds to the one obtained from database[39] (Appendix, Fig. D15).

Intense absorption in the range of 1667 – 1679 cm^{-1} in the IR spectra of the hydrazones (Appendix, Fig. D1 for **H$_2$L^1·MeOH**, Fig. D2 for **H$_2$L^1** and Fig. D3 for **H$_2$L^2**) confirmed the presence of the carbonyl group C=O of the amide tautomer. All ligands exhibited vibration band at *ca.* 1610 cm^{-1} and at *ca.* 1150 cm^{-1} belonging to C=N$_{imine}$ and N–N stretching vibrations of the –(C=O)–NH–N=CH– moiety.[16]

Obtained ligands were analyzed with DSC (Appendix, Fig. D11 for **H$_2$L^1·MeOH**, and Fig. D12 for **H$_2$L^2**). The melting endothermic peaks of all hydrazones are sharp, in narrow temperature interval, directly implying sample purity. The melting point for **H$_2$L^1·MeOH** (after prolonges standing at the room temperature) was at 258 °C and for **H$_2$L^2** was at 252 °C.

4.5. Dioxomolybdenum(VI) complexes

4.5.1. Synthesis and characterization

Mononuclear and polynuclear molybdenum complexes were obtained by the reaction of the corresponding ligand and [MoO$_2$(acac)$_2$] complex (1:1 molar ratio) in absolute methanol or acetonitrile under a reflux condenser. From methanolic solution, orange crystals of the mononuclear complexes **1a** and **2a** were obtained whereas reaction in acetonitrile solution leads to the orange powder of polynuclear complexes **1·MeCN** and **2.** Complex **1** was obtained after 2 hours of heating **1·MeCN** at 120 °C (Scheme 2).
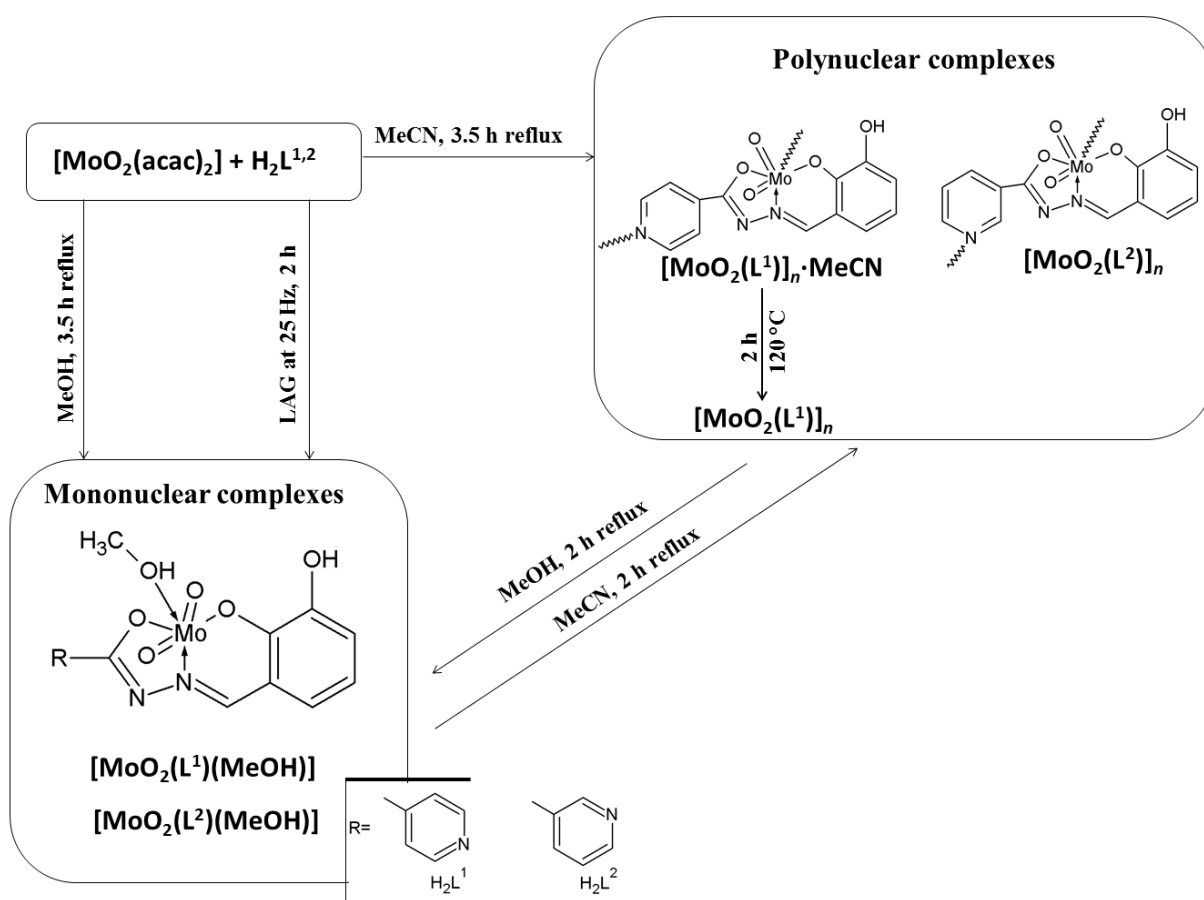
Scheme 2. Synthesis and structural transformations of dioxomolybdenum(VI) complexes.

Orange crystals of complex **1a** were suitable for XRD analysis (Fig. 17). Mo atom displays a slightly distorted octahedral coordination involving a doubly- deprotonated ligand through ONO donor atom set and two oxygen atoms from *cis*-{MoO$_2$}$^{2+}$ unit. The sixth coordination place is occupied with the oxygen atom from a methanol molecule.
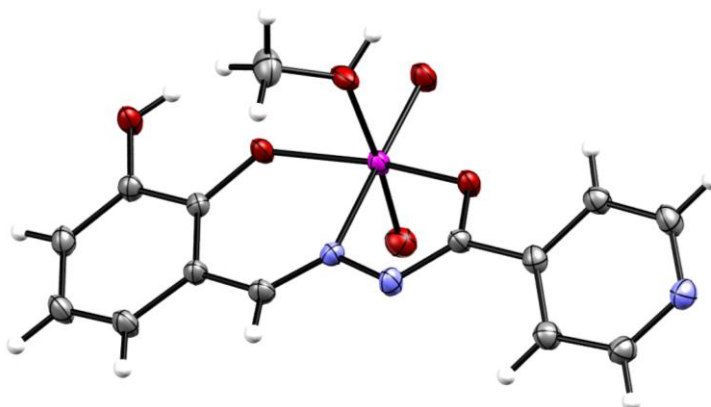
Fig. 17. Molecular structure of complex **1a**.

Successful solid-state synthesis of mononuclear complexes **1a** and **2a** was carried out using the LAG method. Desired products were obtained after 2 hours of ball-milling in the presence of 50 μL of methanol and confirmed with PXRD.

It was possible to transform the mononuclear complexes into the corresponding polynuclear ones by refluxing in acetonitrile for 2 hours. The reversible transformation reaction of the polynuclear into mononuclear complexes in methanol has also been achieved. PXRD diffractograms of complexes with H_2L^1 and H_2L^2 ligands are presented in Appendix, Fig. D16 and Fig. D17, respectively.

All complexes were characterized by IR spectral data. The mononuclear compounds **1a** and **2a** were identified by the appearance of stretching frequencies characteristic for $\nu_{asim}(MoO_2)$ and $\nu_{sym}(MoO_2)$ found at 930 – 933 cm^{-1} and 876 – 880 cm^{-1}. Also, bands around 1030 cm^{-1} and 3300 cm^{-1} are assigned to the C–O and O–H stretching vibrations of the coordinated methanol molecule. In IR spectra of the polynuclear complexes **1** and **2**, vibration corresponding to the cis-$\{MoO_2\}^{2+}$ core is observed at 937 cm^{-1}. The presence of a band around 910 cm^{-1} assigned to $\nu_{asim}(O=Mo–N)$ and absence of a broadband at $ca.$ 850 cm^{-1} characteristic for an intermolecular Mo=O···Mo interaction indicate that polymerisation occurred through a nitrogen atom.[10]

The absorption bands belonging to C=N$_{imine}$ and C–O$_{phenolic}$ groups (at 1599–1612 cm^{-1} and 1564–1576 cm^{-1}, respectively) are present in the spectra of all the complexes. The band typical for C–O group of the hydrazone moiety appears at $ca.$ 1340 cm^{-1}. Those bands are indicative for enol form of ligands and coordination through a deprotonated oxygen atom in all complexes.[9] Polynuclear complexes **1·MeCN** and **1** was not possible to distinguish by IR.

Proton and carbon chemical shifts of complexes **1** and **2** (Appendix, Table. D1) are assigned by using one (^{1}H, ^{13}C-DEPTq) and two-dimensional (COSY, HSQC, HMBC) NMR experiments in DMSO-d_6. Dihidroxybenzaldehyde moiety gave signals in the range 7.22–9.51 ppm for complex **1** and 7.21–9.49 ppm for complex **2**. Signals appeared in ^{1}H spectra at 8.97 ppm for complex **1** and 8.94 ppm for complex **2** are attributed to hydrogen of the CH=N–N group. The ^{13}C NMR spectra of complex **1** show that the pyridine moiety contains two pairs of chemically equivalent carbons (at 121. 99 ppm and 151.10 ppm), while as expected complex **2** does not contain such feature.

NMR spectra of mononuclear complexes **1a** and **2a** were not possible to obtain since DMSO can act as a ligand and coordinate metal center [40].

Molybdenum complexes were analysed by thermogravimetry, under the oxygen atmosphere and within the temperature range from 25 to 600 °C. Residues obtained after thermal decomposition of all complexes are identified with PXRD as molybdenum(VI) oxide MoO_3 (Appendix, Fig. D17).

The thermal analysis data of mononuclear complexes show the first weight loss in the range 131–240 °C (**1a**) and 191–239 °C (**2a**) corresponding to the loss of the coordinated methanol molecule. In the second step (in the range 256–539 °C for **1a** and 265–518 °C for **2a**) the weight loss indicates complex decomposition. When the polynuclear dioxomolybdenum(VI) complex **1·MeCN** is heated in an oxygen atmosphere the first weight loss starts around 27 °C is attributed to the loss of crystallised acetonitrile molecule, which is simultaneously followed by the complex decomposition in the range 283–491 °C. Thermogravimetric curves for the polynuclear complexes **1** and **2** show decomposition in one step and the weight loss in the range 243–517 °C and 196–538 °C, respectively. The gray residue after termal decomposition of polynuclear complexes also corresponds to the MoO_3.

4.6. Molybdenum(VI) complexes as catalysts in the oxidation reactions of secondary alcohols

Oxidation of secondary alcohols carveol and cyclohexanol catalyzed by molybdenum (VI) complexes **1**, **2**, **1a** and **2a** have been studied. The effects of various factors, such as 1) oxidant TBHP (aqueous solution and in decane) *vs.* H_2O_2,) substituent on the ligand − the influence of isoniaside *vs.* nicotinic acid hydrazide and 3) type of complex (polynuclear *vs.* mononuclear) have been investigated.

The reactions were carried out at 80 °C in a stirred solution of the substrate, catalyst and oxidant in acetonitrile for 5 h. All the complexes were insoluble in acetonitrile at room temperature (orange slurry) but dissolved after 150 minutes in carveol reaction mixture or after 20 minutes in cyclohexanol reaction mixture at 80°C (orange mixture turn yellow until the end of the reaction). Aliquots were withdrawn from the reaction mixture, diluted with acetonitrile and injected into GC apparatus. The conversion of substrates and the formation of products were calculated according to an internal standard, acetophenone. The values are expressed in terms presented in Chapter 2.4.1.

4.6.1. Carveol oxidation

As already stated in Chapter 2.4.3., in catalytic oxidation of the mixture *cis-* and *trans-* carveol desired product is carvone. In order to find efficient and eco-friendlier catalytic system reactions were conducted with low Mo loading (n(Mo in complex) : n(alcohol) = 0.025 mmol : 10 mmol) in the presence of H_2O_2 or TBHP (aqueous solution or solution in decane), (n(oxidant) : n(alcohol) = 10 mmol : 20 mmol).

In the case of H_2O_2, the conversion of carveol is high (84–87 %) for all tested molybdenum complexes, following the order **2a** < **1** < **1a** ~ **2**. In the presence of aqueous TBHP complexes show moderate to good conversions (56–66 %) in the order **2a** < **1a** < **1** < **2**. Kinetic profiles of the reactions are presented in Fig. 18 and 19.
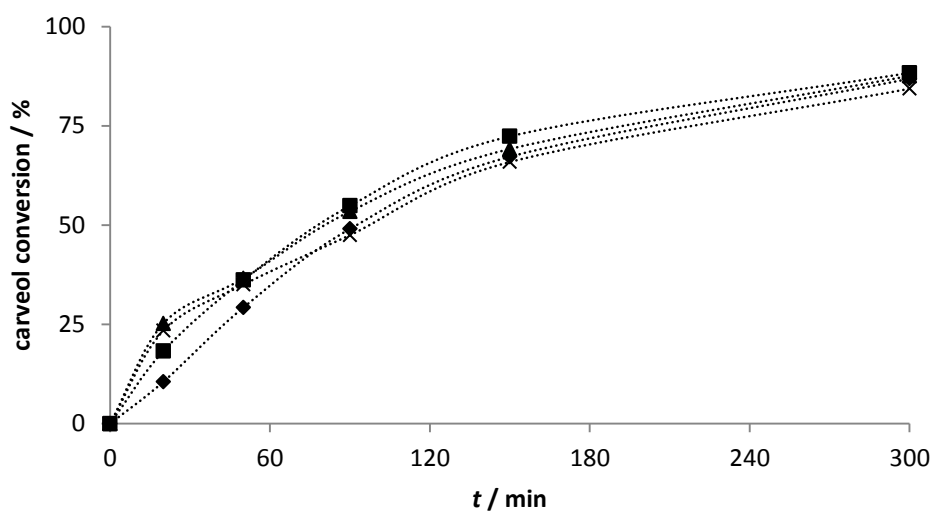
Fig. 18. Converted carveol *vs.* time with molybdenum(VI) (pre)catalyst ♦ complex **1**, ■ complex **1a**, ▲ complex **2**, × complex **2a**. Conditions: n(Mo) : n(substrate) : n(H$_2$O$_2$) = 1 : 400 : 800, T = 353 K.
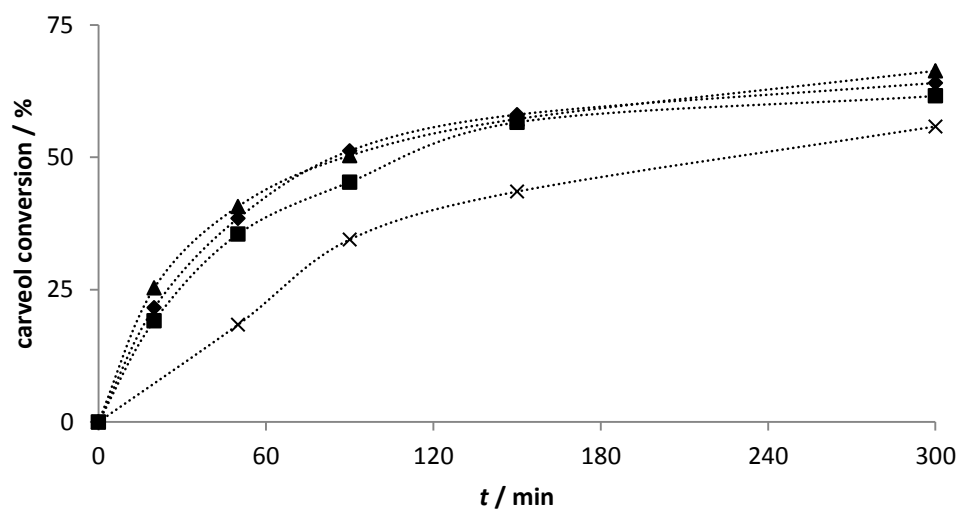
Fig. 19. Converted carveol *vs.* time with molybdenum(VI) (pre)catalyst ♦ complex **1**, ■ complex **1a**, ▲ complex **2**, × complex **2a**. Conditions: n(Mo) : n(substrate) : n(TBHP$_{aq}$) = 1 : 400 : 800, T = 353 K.

In catalytic system with H$_2$O$_2$, all catalysts show similar values of selectivities (41–42 %), with moderate ketone yield after 5 h (35 – 37 %) (Fig. 20).

On the other hand, low selectivity towards carvone (10–19 %) with low yield (6–11%) were reported for all catalytic reactions with aqueous TBHP. Interestingly, complex **2a** with

aqueous TBHP shows the lowest carveol conversion (56 %), but the highest selectivity towards carvone (19 %) and carvone yield (11 %) compared to other catalysts (selectivity at *ca.* 10 % and yield at *ca.* 7 %) (Fig. 21). A slower rate of reaction seems to be in favor of carvone formation.

Fig. 20. Results of the carveol oxidation catalyzed with molybdenum(VI) complexes in the presence of H_2O_2 after 5 h. (n(Mo) : n(substrate) : n(H_2O_2) = 1 : 400 : 800, T = 353 K). Carvone selectivitiy (dark cylinders); carvone yield (light cylinders).
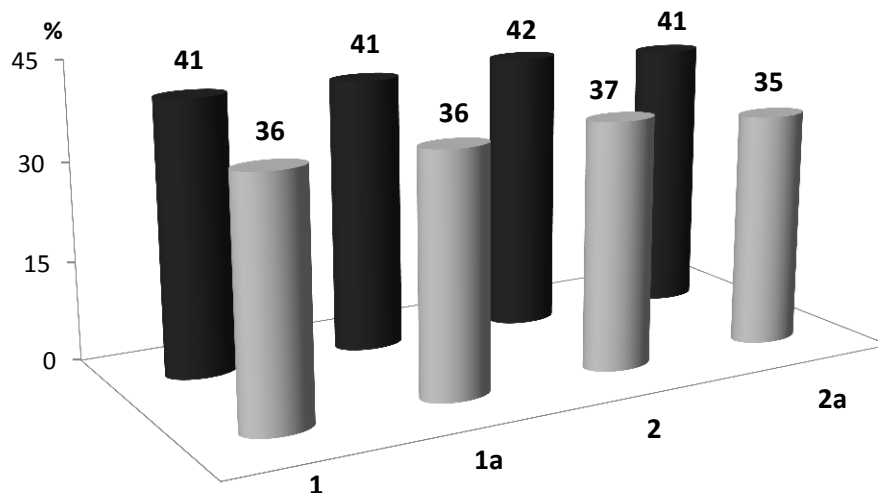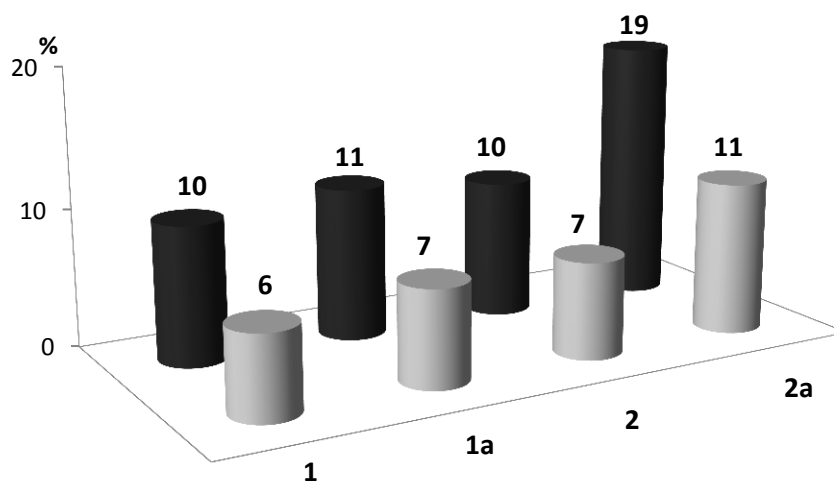

Fig. 21. Results of the carveol oxidation catalyzed with molybdenum(VI) complexes in the presence of aqueous TBHP after 5 h.(n(Mo) : n(substrate) : n($TBHP_{aq}$) = 1 : 400 : 800, T = 353 K). Carvone selectivity (dark cylinders); carvone yield (light cylinders).

Additionally, catalytic activity of the complex **2a** was tested in the presence of TBHP solution in decane and remarkable carveol conversion is achived (99 %) (Fig. 22). However, due to low selectivity towards carvone (4 %) (Table 1), further testing of other complexes was not performed under these conditions.
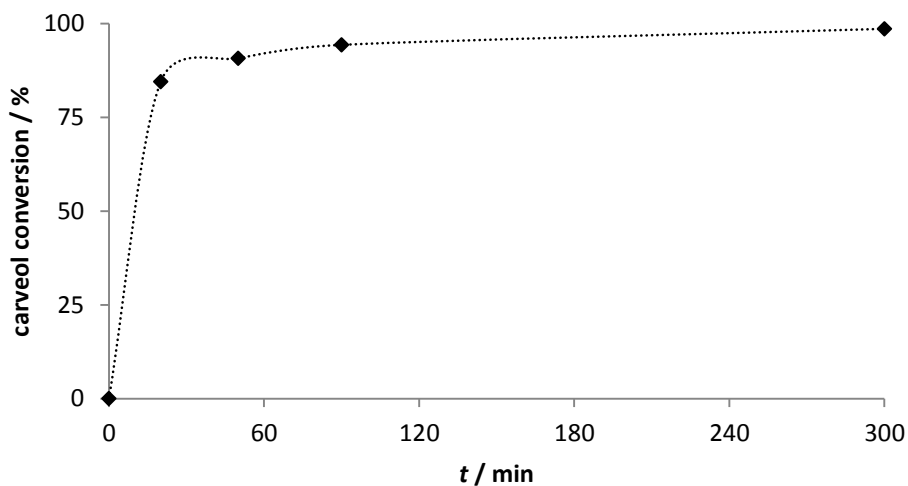
Fig. 22. Converted carveol *vs.* time with molybdenum(VI) complex **2a**. Conditions: n(Mo) : n(substrate) : n(TBHP$_{decane}$) = 1 : 400 : 800, T = 353 K.

All relevant catalytic data are presented in Table 1. Initial turnoever frequencies (TOF$_{20min}$) for all tested molybdenum catalysts with H$_2$O$_2$ and TBHP aqueous solutions are relatively low, which implies a slower activation time of the complexes. Considering that the conversion of carveol in the case of TBHP solution in decane after 20 min was extremely high (84 %), it is not surprising that TOF also achieved high value, 1001 h^{-1}.

Table 1. Results of the carveol oxidation catalyzed with molybdenum(VI) complexes under following conditions n(Mo) : n(substrate) : n(oxidant) = 1 : 400 : 800, T = 353 K.

	Conversion (carveol) / %	Selectivity (carvone) / %	TOF$_{20min}$ / h^{-1}	TON
H$_2$O$_2$				
1	88	41	113	308
1a	87	41	23	36
2	87	42	294	339
2a	84	41	286	344
TBHP (aqueous solution)				
1	64	10	237	235
1a	62	11	29	27
2	66	10	29	27
2a	56	19	185	271
TBHP (solution in decane)				
2a	99	4	1001	289

Since carveol contains two double bonds that may be targeted by the oxidant, it is not surprising that the relatively high conversion of carveol is accompanied by low selectivity towards carvone. Most likely, carveol epoxidation can occur, and two types of carveol epoxides [28] can be yielded. Also, low carvone yield can be explained due to formation of the carvone epoxides [41-43] . (Fig. 24)
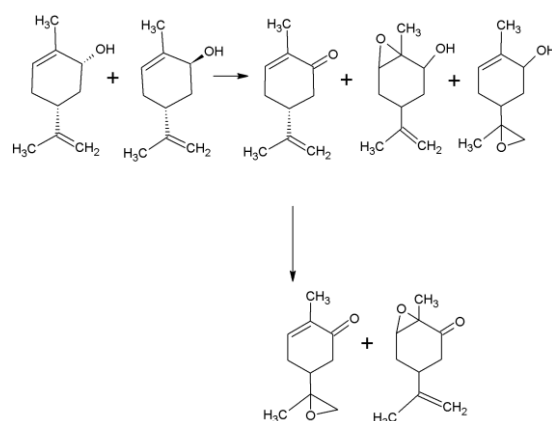

Fig. 24. Oxidation scheme for carveol and carvone.

From the obtained results it can be seen that the substituent on the ligand (isoniaside *vs.* nicotinic acid hydrazide) and type of complex (polynuclear *vs.* mononuclear) do not have much influence on oxidation of carveol. However, the influence of the used oxidant on the selectivity towards carvone should be discussed.

During the reaction, a different consumption of *cis-* and *trans-* carveol was observed in the GC spectra for each of the oxidants. Keeping that in mind, the different selectivity towards carvone can be explained by reaction stereoselectivity towards *cis-* or *trans-* carveol. By NMR analysis [44] of the obtained reaction mixtures, it was determined that in the presence of H_2O_2 as oxidant, the prefered substrate is *cis*-carveol, while if aqueous TBHP is used, the prefered substrate is *trans*–carveol (Fig. 25). Concluding, the oxidation of *cis-* carveol seems to lead to the formation of the desired product, carvone, which makes H_2O_2 a better oxidant for this catalytic reaction.
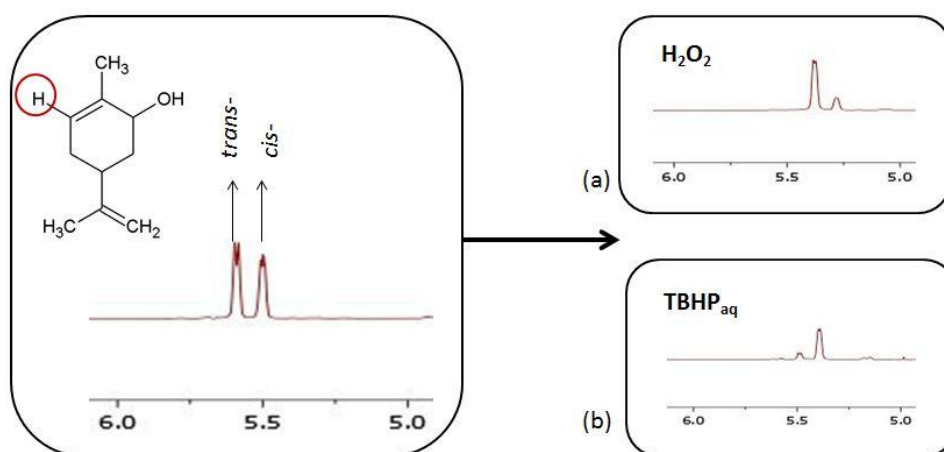
Fig. 25. The relevant part of the NMR spectra (Appendix, Fig. D23):(left) mixture of *cis-* and *trans-* carveol, reaction mixture with (a) H_2O_2 or (b) $TBHP_{aq}$ in the presence of complex **2**.

In addition, high peak belonging to an unknown compound **A** was observed in the GC spectra. In reaction mixture with H_2O_2, carvone is the main product and compound **A** is a by-product. In contrast, unknown compound **A** is the main product if TBHP (in aqueous solution or solution in decane) is used as oxidant. Furthermore, GC and NMR spectra indicated more than two by-products in all types of reaction conditions.

In order to identify by-products, several experiments were performed. After purification by column chromatography[i] of the the reaction mixtures with H_2O_2 and TBHP in aqueous solution, the obtained fractions were analyzed by GC-MS, NMR and GC.

Unfortunately, it was not possible to identify the unknown product **A** with certainty. In GC-MS experiment product **A** was identified as limonene diepoxide whose presence was not confirmed in the NMR spectra. Besides, limonene diepoxide is not the most likely product in this reaction.[45] The fraction in which product **A** was isolated was contaminated with other by-products and due to overlaping of the NMR peaks, no identification was possible. Moreover, NMR spectra for all probable compounds and their isomers, *e. g.* carveol and carvone epoxides have not been found in the literature. In order to identify unknown compound **A**, additional investigations are needed.

GC-MS spectral data additionally confirmed the previously assumed stereoselectivity of the reaction towards *cis*-carveol in case H_2O_2 and towards *trans*-carveol in the case of TBHP in aqueous solution.

4.6.2. Oxidation of cyclohexanol

Cyclohexanone, an important precursor in the production of nylon 6 and nylon 66 (see Chapter 2.4.4.) is the expected oxidation product of cyclohexanol. In order to find favorable catalytic conditions, the use of different oxidants, as well as different catalyst loading was investigated.

At first, reactions were conducted with low Mo loading (n(Mo in complex) : n(alcohol) = 0.025 mmol : 10 mmol) in the presence of H_2O_2 or TBHP (aqueous solution or solution in decane), (n(oxidant) : n(alcohol) = 10 mmol : 20 mmol). Since cyclohexanol conversion was low, no further testing with complexes **1** and **1a** were performed under these conditions.

Complex **2** and **2a** were tested as catalysts with H_2O_2 (Fig. 26) and conversion in the first 150 minutes of the reaction is extremley low. Despite low cyclohexanol conversion values (11 % for **2** and 13 % for **2a**, after 5 h), selectivity towards cyclohexanol is moderate (64 % for **2** and 59 % for **2a**).

---

[i] Conditions for CC: Stationary phase: silica gel. Mobile phase: 250 mL of the mixtures of hexane and diethyl ether with different polarities (diethyl ether content: 5 %, 10 %, 10 %, 30 %, 50 %, 100 %). The composition of the eluent flow was monitored with TLC and visualized with UV lamp, iodine or permanganate.
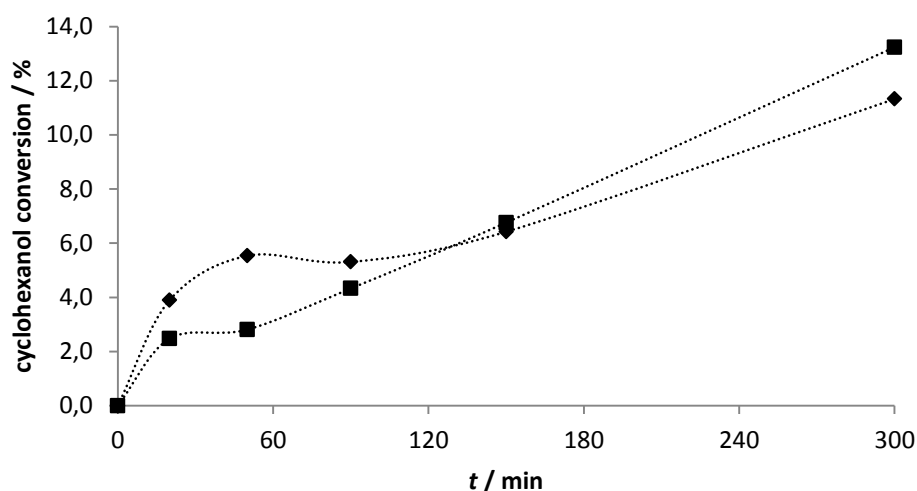
Fig. 26. Converted cyclohexanol *vs.* time with molybdenum(VI) (pre)catalyst ♦ complex **2**, ■ complex **2a**. Conditions: $n(Mo) : n(substrate) : n(H_2O_2) = 1 : 400 : 800$, $T = 353$ K.

All relevant catalytic data are presented in Table 2. A catalytic system with complex **2a** and TBHP solution in the decane provides the highest cyclohexanol conversion (28 %) and cyclohexanone yield (16 %), while the selectivity towards cychlohexanone is the same as with H_2O_2 (59 %).

Table 2. Results of the cyclohexanol oxidation catalyzed with molybdenum(VI) complex **2** and **2a** in the presence of different oxidants after 5 h ($n(Mo) : n(substrate) : n(oxidant) = 1 : 400 : 800$, $T = 353$ K).

	Conversion (cyclohexanol) / %	Formation (cyclohexanone) / %	Selectivity (cyclohexanone) / %
2			
H_2O_2	11	7	64
2a			
H_2O_2	13	8	59
TBHP$_{aq}$	17	5	31
TBHP$_{decane}$	28	16	59

The impact of higher catalyst loading was also investigated. In order to follow the principles of green catalysis, higher catalyst loading is accompanied by a lower content of oxidant. All molybdenum(VI) complexes were tested within the following reaction conditions: (n(Mo in complex) : n(alcohol) = 0.05 mmol : 5 mmol) in the presence of H_2O_2 (n(oxidant) : n(alcohol) = 15 mmol : 5 mmol).

A significant conversion of cyclohexanol is now evident after 90 minutes of reaction (Fig. 27). Slightly higher conversion is also achieved after 5 h (15 − 21 %), following the order **2** < **2a** < **1** < **1a**. Higher values of selectivity were also observed, the lowest being 59 % for complex **1** and the highest one 71 % for complex **2** (Fig. 28). Furthermore, cyclohexanone yield is between 11–14 % (Table 3).

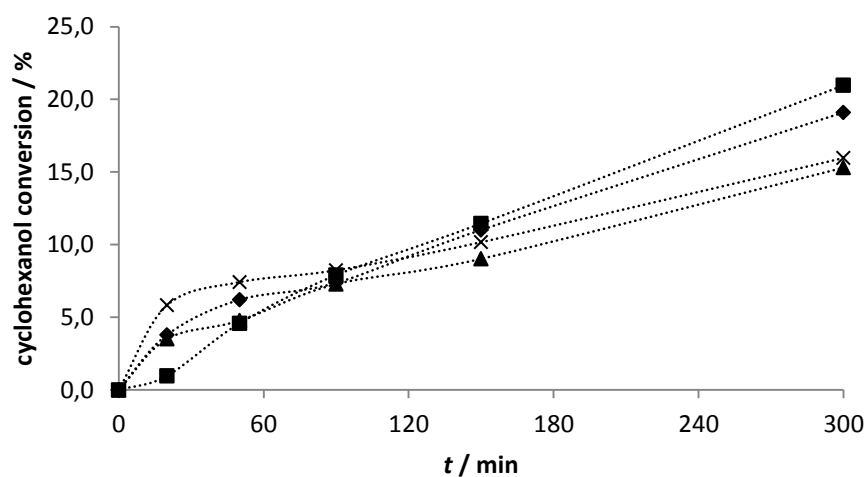Fig. 27. Converted cyclohexanol *vs.* time with molybdenum(VI) (pre)catalyst ♦ complex **1**, ■ complex **1a**, ▲ complex **2**, × complex **2a**. Conditions: n(Mo) : n(substrate) : n(H$_2$O$_2$) = 1 : 100 : 300, T = 353 K

Table 3. Results of the cyclohexanol oxidation catalyzed with molybdenum(VI) complexes in the presence of H_2O_2 after 5 h (n(Mo) : n(substrate) : n(oxidant) = 1 : 100 : 300, T = 353 K).

	Conversion (cyclohexanol) / %	Formation (cyclohexanone) / %	Selectivity (cyclohexanone) / %
1	19	11	59
1a	21	14	66
2	15	11	71
2a	16	11	66

The substituent on the ligand (isoniaside *vs*. nicotinic acid hydrazide) and type of complex (polynuclear *vs*. mononuclear) do not have much influence on the oxidation of cyclohexanol. However, higher catalyst loading provides better results and further investigations should be carried out under these conditions in the presence TBHP (aqueous solution and solution in decane) to determine the exact influence of oxidant. Current research indicates that TBHP solution in decane might be more suitable oxidant than H_2O_2 or TBHP in aqueous solution under these catalytic conditions.

§ 5.   CONCLUSION

In the first step of this diploma thesis, hydrazone based ligands **H₂L¹·MeOH** and **H₂L²** have been synthesized in condensation reactions between 2,3-dihydroxybenzaldehyde and isonicotinic or nicotinic hydrazide, in dry methanol. Furthermore, successful solid state synthesis of the **H₂L¹** ligand was carried out using the LAG method and synthesis progress was followed *ex–situ* with PXRD method. Keto tautomeric form of both ligands is indicated from IR spectroscopy data, while this information is additionally supported for ligand **H₂L¹·MeOH** from its crystal structure.

Secondly, reactions performed with $[MoO_2(acac)_2]$ as starting compound and appropriate ligand (**H₂L¹** or **H₂L²**) in acetonitrile lead to the formation of polynuclear complexes $[MoO_2(L^1)]_n \cdot MeCN$ and $[MoO_2(L^2)]_n$. $[MoO_2(L^1)]_n$ was possible to obtain after 1 hour of heating of complex $[MoO_2(L^1)]_n \cdot MeCN$ at 110 °C. On the other hand, reactions carried out in methanolic solution or in solid-state (LAG method) resulted in the formation of mononuclear complexes $[MoO_2(L^1)MeOH]$ and $[MoO_2(L^2)MeOH]$. Also, reversible strucutral transformations between polynuclear and mononuclear complexes are observed by refluxing in appropriate solvent. In all complexes, hydrazone ligand is coordinated to the *cis*-$\{MoO_2\}^{2+}$ core through ONO donor atom set. The sixth coordination site is occupied by the nitrogen atom from hydrazone moiety from neighboring complex or by methanol molecule.

At last, molybdenum(VI) complexes were tested as catalysts in the oxidation of secondary alcohols, carveol and cyclohexanol in the presence of different oxidants, H_2O_2 and TBHP (in aqueous solution or solution in decane). Oxidation of carveol occurred with very good conversions. However, carvone yield was better with H_2O_2 and it can be compared to the results previously reported in the literature[28, 29]. Generally speaking, low selectivity towards carvone can be explained due to transformation of *trans*-carveol into unknown compounds. Also, yielded carvone was partially lost as carvone epoxide. Catalytic tests for cyclohexanol were less successful and require further optimization of reaction conditions. Although the reaction is relatively slow, selectivity towards cyclohexanone makes this catalytic system potentially applicable in the future.   Since the complexes with different ligands substituents showed similar kinetic parameters, the general conclusion was that the ligand influence on the catalysis is not significant, as well as the type of used complex (mononuclear or polynuclear).

§ 6.   LIST OF ABBREVIATIONS AND SYMBOLS

acac   acetylacetonate

CC   column chromatography

DMSO   dimethyl sulfoxide

DSC   differental scanning calorimetry

GC   gas chromatography

IR   infrared

L   ligand (generalized)

NMR   nuclear magnetic resonance

MeCN   acetonitrile

MeOH   methanol

PXRD   powder X-ray diffraction

TBHP   *tert*-butyl hydroperoxide

TG   thermogravimetry

TLC   thin layer chromatography

TOF   turn-over frequency

TON   turn-over number

XRD   X-ray diffraction

§ 7. REFERENCES

1. X. Su, I. Aprahamian, *Chem. Soc. Rev*. **43** (2014) 1963-1981.

2. H. A. Rudbari, M. Khorshidifard, B. Askari, N. Habibi, G. Bruno, *Polyhedron* **100** (2015) 180-191.

3. A. Schabauer, C. Zutz, B. Lung, M. Wagner, K. Rychil, *Front. Vet. Sci*. **148** (2018).

4. H. Adibi, S. Zaker, H. Monakaresi, *JRPS* **1** (2012) 60-66.

5. K. S. Abou-Melha, *Spectrochimica Acta Part A* **70** (2008) 162-170.

6. S. R. Gupta, P. Mourya, M. M. Singh, V. P. Singh, *Journal of Molecular Structure* **1137** (2017) 240-252.

7. R. R. Mendel, *Dalton Trans.* **21** (2005) 3404-4309.

8. R. Hille, *Chem. Rev.* **96** (1996) 2757-2816.

9. J. Pisk, B. Prugovečki, D. Matković-Čalogović, T. Jednačak, P. Novak, D. Agustin, V. Vrdoljak, *RSC Adv.* **4** (2014) 39000-39010.

10. V. Vrdoljak, B. Prugovečki, I. Pulić, M. Cigler, D. Sviben, J. Parlov Vuković, P. Novak, D. Matković-Čalogović, M. Cindrić, *New J. Chem.* **39** (2015) 7322-7332.

11. V. Vrdoljak, M. Mandarić, T. Hrenar, I. Đilović, J. Pisk, G. Pavlović, M. Cindrić, D. Agustin, *Cryst. Growth Des.* **19** (2019) 3000-3011.

12. K. Nakajima, K. Yokoyama, T. Kano, M. Kojima, *Inorg. Chim. Acta* **282** (1981) 209–216.

13. R. D. Chakravarty and D. K. Chand, *J. Chem. Sci.* **132** (2011) 187–199.

14. N. R. Rightmire, T. P. Hanusa, *Dalton Trans.* **45** (2016) 2352-2362.

15. *IUPAC. Compendium of Chemical Terminology,* 2nd ed. (the "Gold Book"). Compiled by A. D. McNaught and A. Wilkinson. Blackwell Scientific Publications, Oxford (1997). Online version (2019-) created by S. J. Chalk. ISBN 0-9678550-9-8. https://doi.org/10.1351/goldbook, https://goldbook.iupac.org/terms/view/MT07141 (datum pristupa 8. kolovoza 2019.).

16. J. Pisk, T. Hrenar, M. Rubčić, G. Pavlović, V. Damjanović, V. Lovrić, M. Cindrić, V. Vrdoljak, *CrystEngComm* **20** (2018) 1804-1817.

17. R. A. Sheldon, I. Arends, U. Hanefeld, *Green Chemistry and Catalysis*, Wiley-VCH, Weinheim, 2007, str. 1-2.

18. X. Wu, F. Li, B. Zhang, L. Sun, *Journal of Photochemistry and Photobiology C: Photochemistry Reviews* **25** (2015) 71-89.

19. J. W. Wang, W. J. Liu, D. C. Zhong, T. B. Lu, *Coordination Chemistry Reviews* **378** (2019) 237-261.

20. S. Liu, Y. J. Lei, Z. J. Xin, Y. B. Ly, H. Y. Wang, *Journal of Photochemistry and Photobiology* A*: Chemistry* **355** (2018) 141-151.

21. M. Campanati, G. Fornasari, A. Vaccari, *Catalysis Today* **77** (2003) 299-314.

22. B. Guérin, D. M. Fernandes, J.-C. Daran, D. Agustin, R. Poli, *New J. Chem.* **37** (2013) 3466-3475.

23. J. M. Brégeault, J. Chem. Soc., *Dalton Trans.* **30** (2003) 3289–3302.

24. S. P. Bhatia, D. Mcginty, C. S. Letizia, Am. M. Api, *Food and Chemical Toxicology* **46** (2008) 85-87.

25. M. Stekrova, N. Kumar, S. F. Díaz, P. Mäki-Arvela, D. Yu. Murzin, *Catalysis Today* **241** (2015) 237-245.

26. J. A. Becerra. L. M. Gonález, A. L. Villa, *Catalysis Today* **302** (2018) 250-260.

27. J. Młodzik, A. Wróblewska, E. Makuch, R. J. Wróbel, *Catalysis Today* **268** (2016) 111-120.

28. I. Santos, J. Gamelas, T. Duarte, M. Simoes, M. Neves, J. Cavaleiro, A. Cavaleiro, *Journal of Molecular Catalysis A: Chemical* **426** (2017) 593-599.

29. D. Grajales, L. Gonzáles, A. Villa, *Applied Catalysis A, General* **541** (2017) 15-24.

30. M. T. Musser, *Cyclohexanol and Cyclohexanone in: Ullmann´s Encyclopedia of Industrial Chemistry*, Wiley-VCH, 2011.

31. F. Cavani, L. Ferroni, A. Frattini, C. Lucarelli, A. Mazzini, K, Raabova, S. Alini, P. Accorinti, P. Babini, *Applied Catalysis A: General* **391** (2011) 118-124.

32. S. Mouanni, T. Mazari, D. Amitouche, S. Bendji, L. Dermeche, C. Roch-Marchal, C. Rabia, C. R. Chimie **22** (2019) 327-336.

33. R. Hajavazzadadeh, M. K. Zazi, A. R. Mahjoub, *Int. J. Nano Dimens* **10** (2019) 69-77.

34. C. Soumini, S. Sugunan, S. Haridas, *Journal of Porous Materials* **26** (2019) 631-640.

35. Z. Hao, Y. Li, C. Li, R. Wu, Z. Ma, S. Li, Z. Ha, X. Zheng, J. Lin*, Applied Organometallic Chemistry*, **33** (2019) 4750-4759.

36. M. R. Maurya, S. Dhaka, F. Avecilla, *New J. Chem*. **39** (2015) 2130-2139.

37. M. R. Maurya, N. Saini, F. Avecilla, *Inorganica Chimica Acta* **438** (2015) 168-178.

38. E. Tecer, N. Dege, A. Zülfikaroglu, N. Şenüz, *Acta Cryst.* **66** (2010) 2269-3370.

39. N. Dege, N. Şenyüz, N. Günay, Ö. Tamer, Y. Atalay, *Spectrochimica Acta Part A: Molecular and Biomolecular Spectroscopy* **120** (2014) 323-331.

40. M. Calligaris, *Coordination Chemistry Reviews* **248** (2004) 351-375.

41. J. P. Feng, Z. Shi*, J. Org. Chem.* **73** (2008) 6873–6876.

42. X. L. Qi, J. T. Zhang, J. P. Feng, X. P. Cao, Org*. Biomol. Chem.* **9** (2011) 3817-3824.

43. K. K. W. Mak, Y. M. Lai, Y. H. Siu, *Journal of Chemical Education* **83** (2006) 1058-1061.

44. Z. Rafiński, J. Ścianowski, *Tetrahedron: Asymmetry* **19** (2008) 1237–1244.

45. J. Cubillos, S. Vásquesm, C. M. Correa, *Applied Catalysis A: General* **373** (2010) 57-65.

46. L. Kihlborg*, Arkiv för Kemi*, **21** (1963) 357-364.

47. L. H. K. Queiroz, V. Lacerda , R. B. Santos, S. J. Greco, A. C. Neto , E. V. R. de Castro, *Magn. Reson. Chem.* **49** (2011) 140–146.

§ 8.   APPENDIX
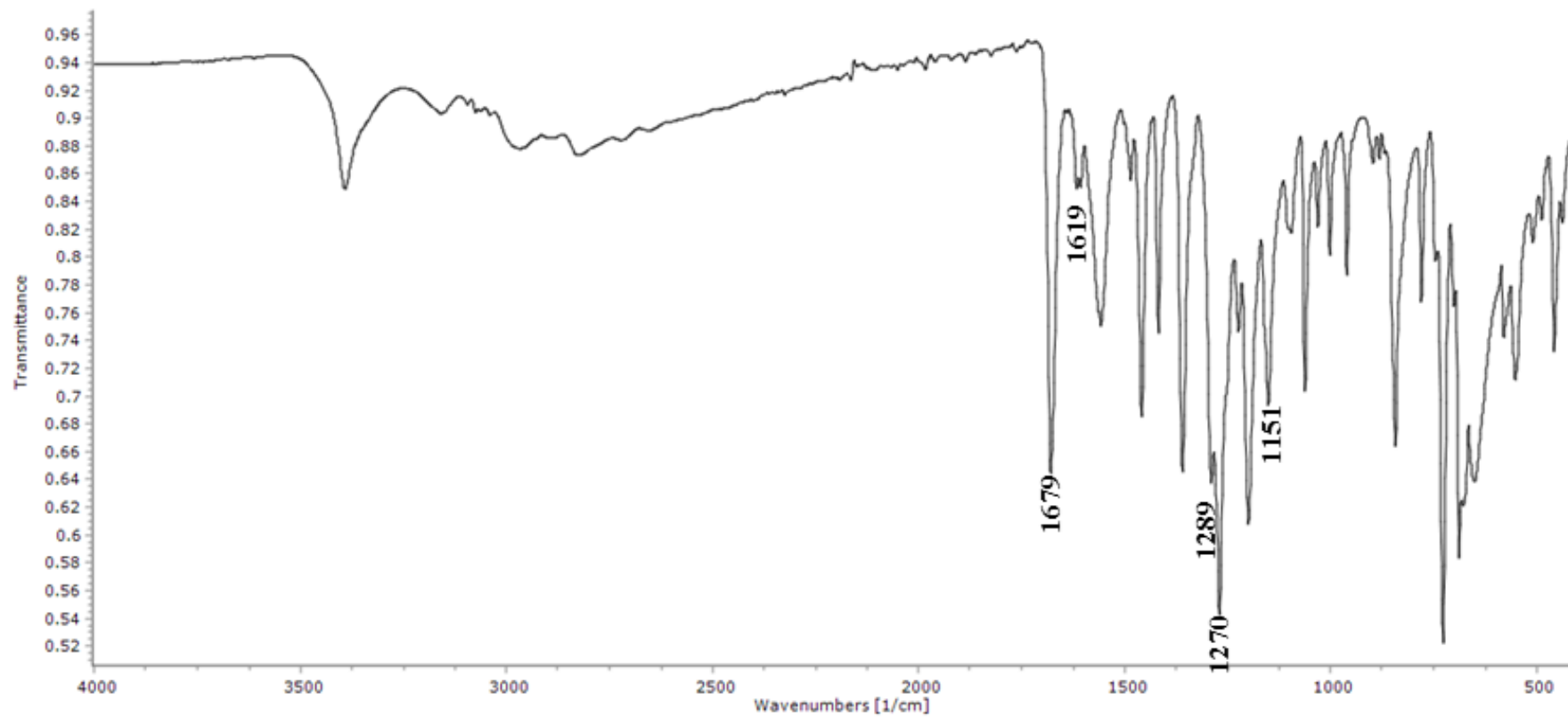
Figure D1. IR spectra of the ligand **H₂L¹·MeOH** (solution based synthesis).
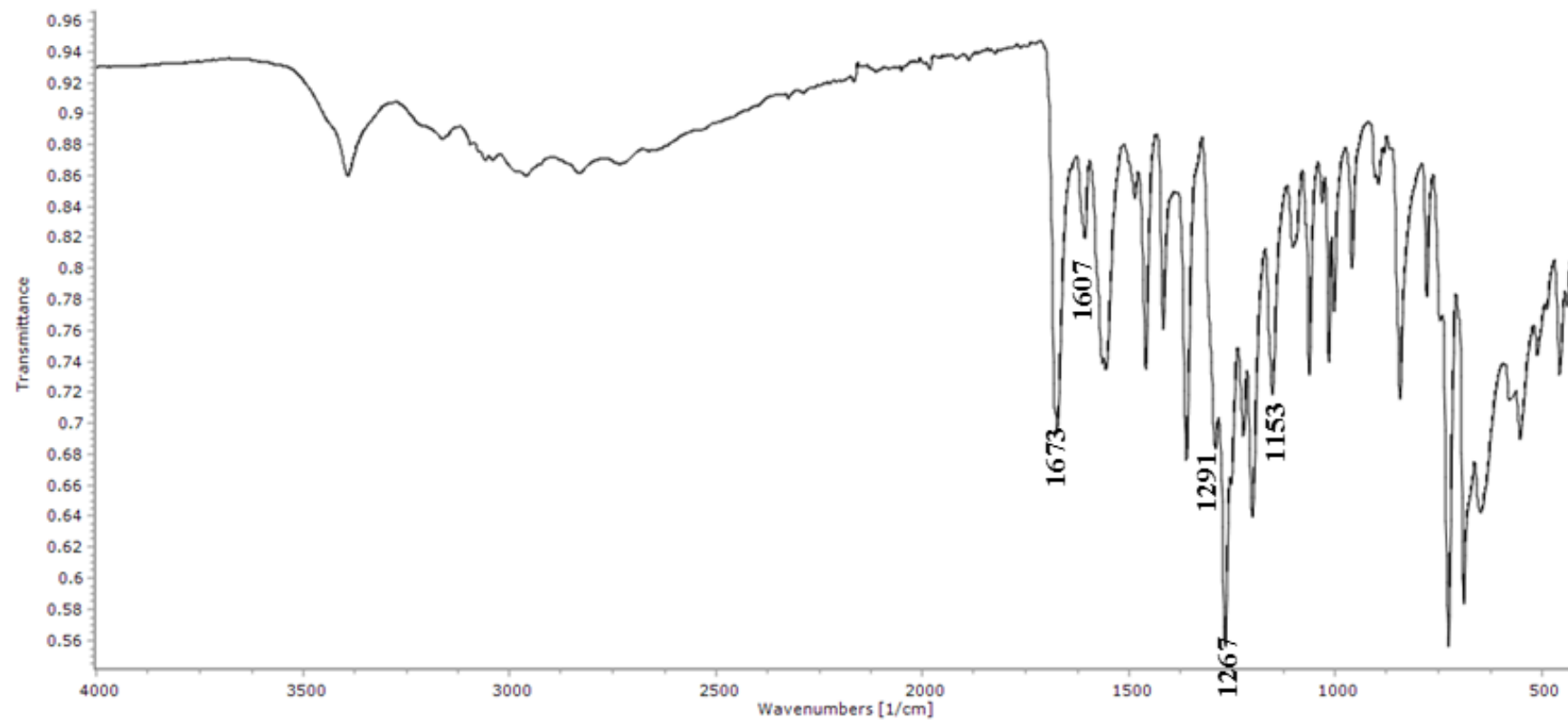
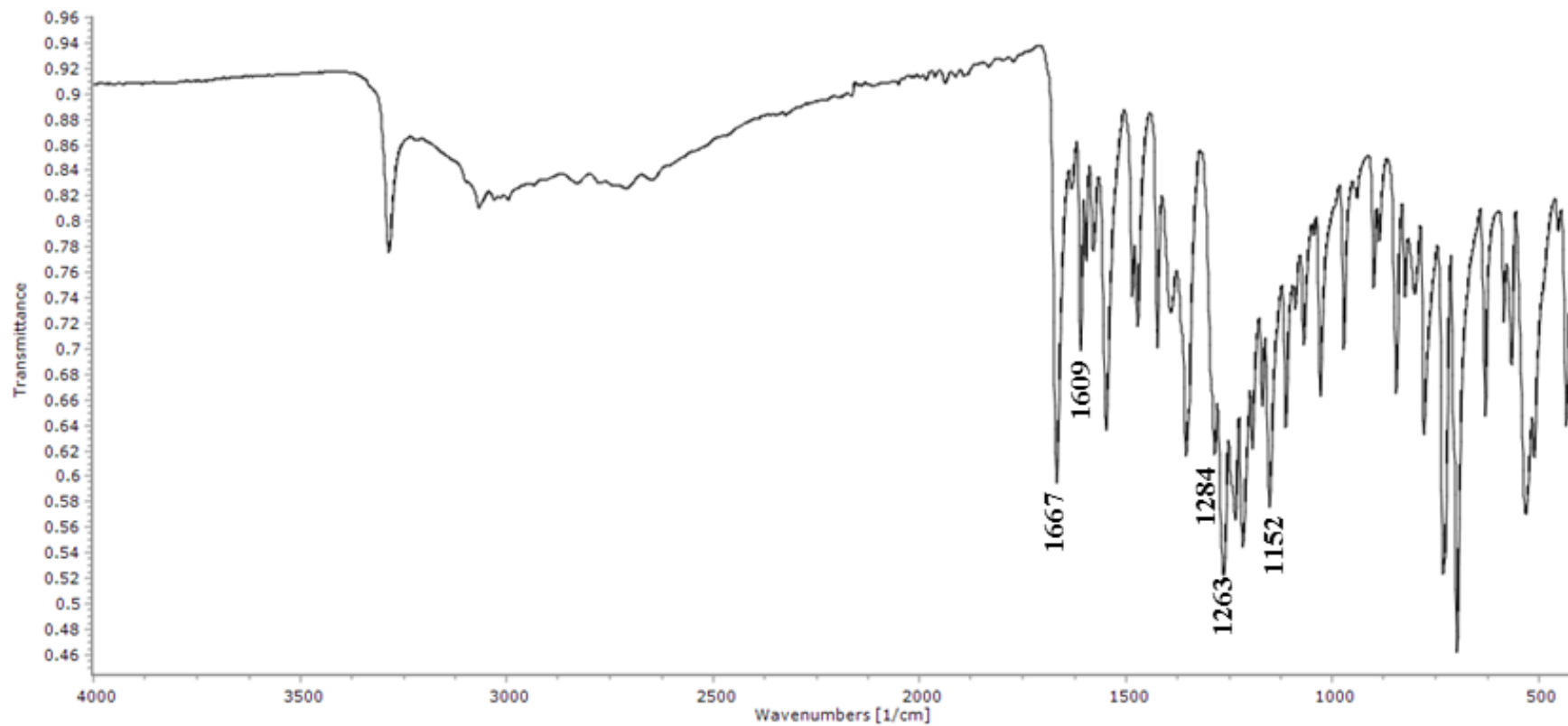Figure D2. IR spectra of the ligand H_2L^1 (mechanochemical synthesis).

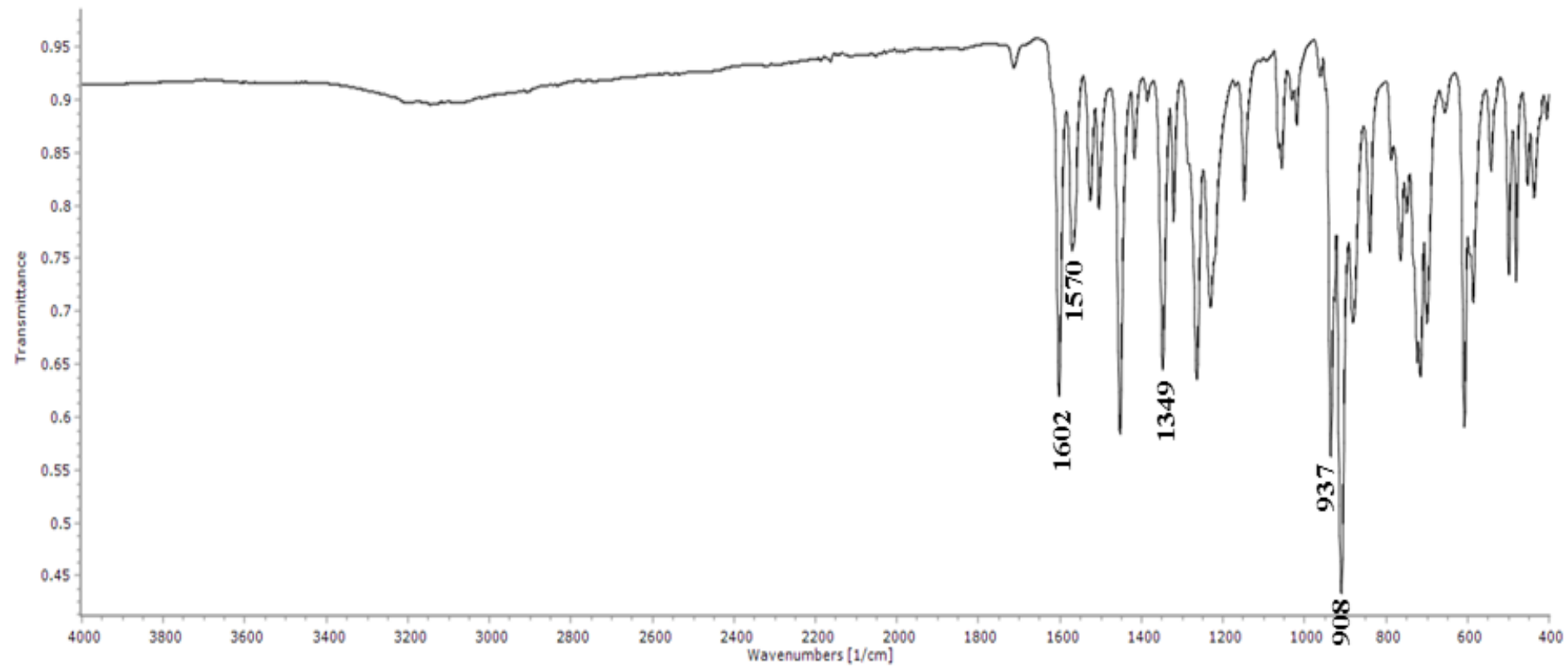Figure D3. IR spectra of the ligand **H₂L²**.

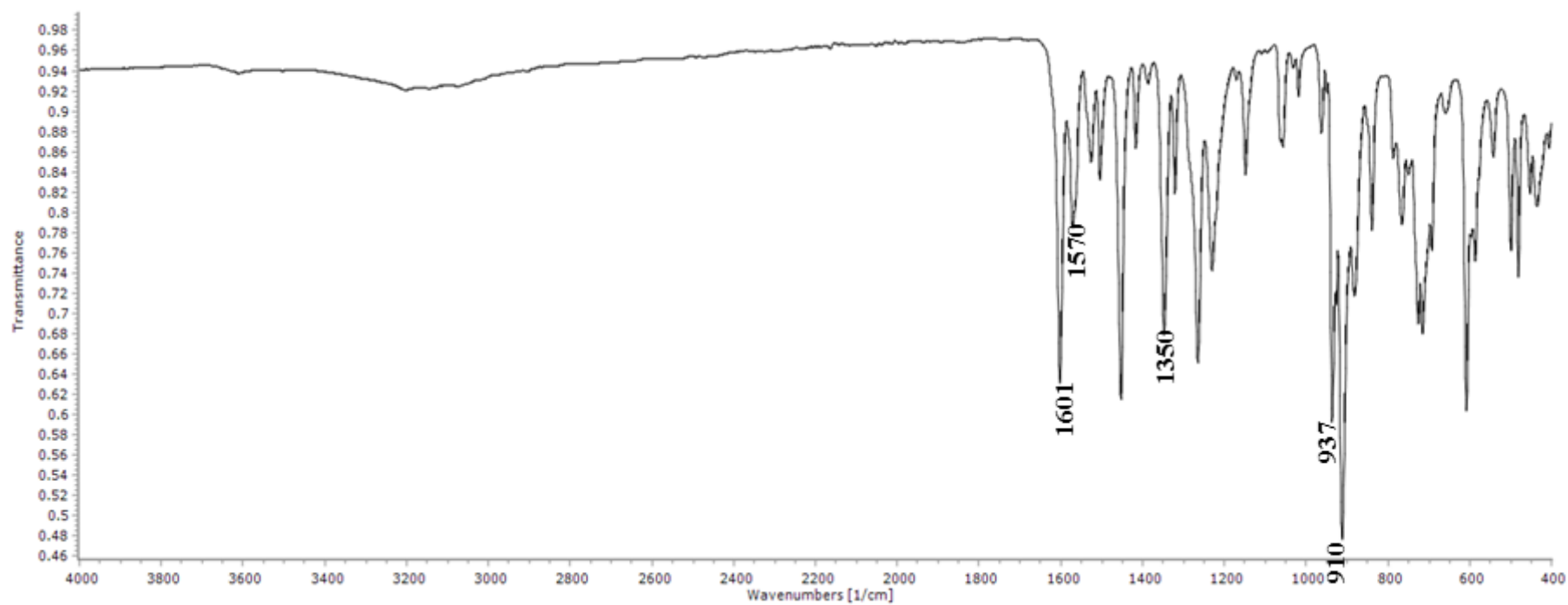Figure D4. IR spectra of the complex **1·MeCN.**
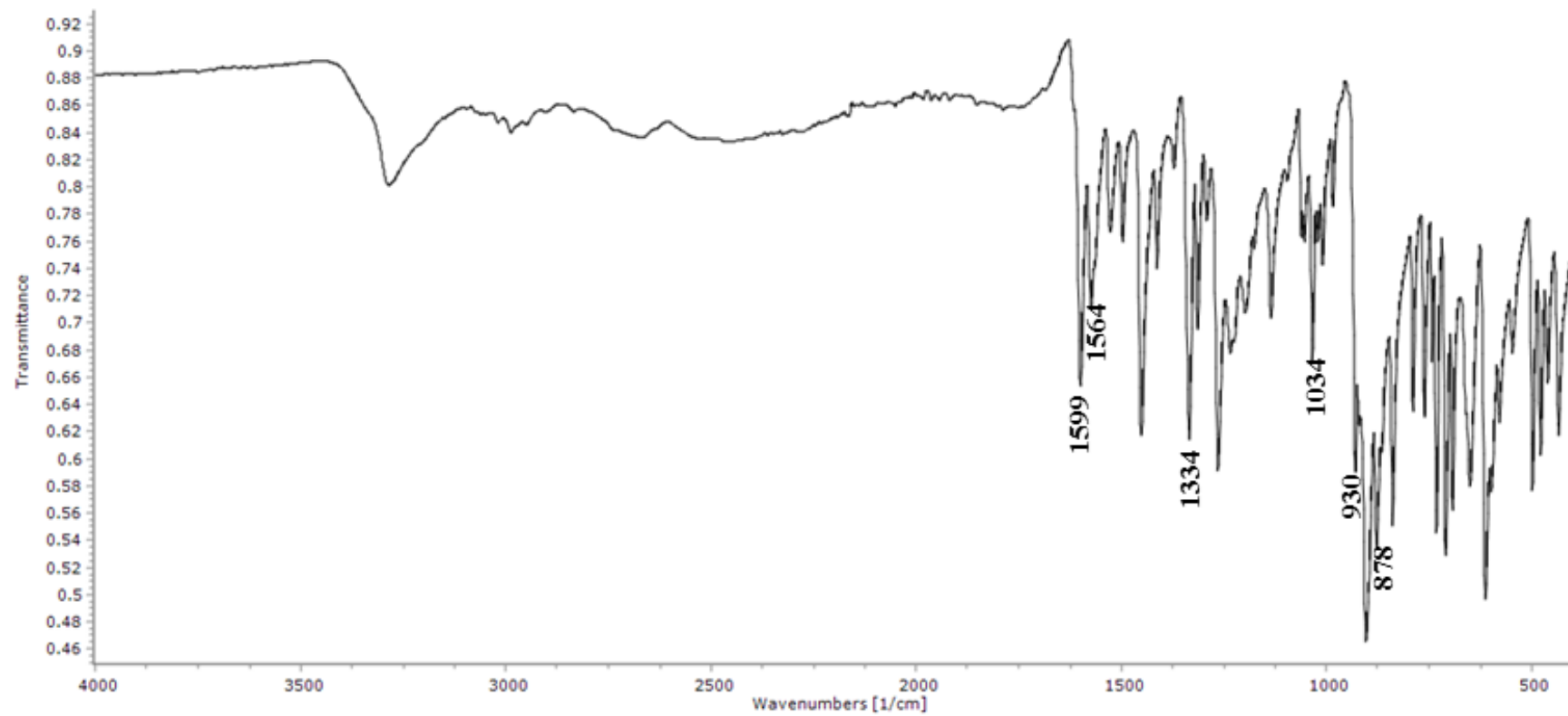
Figure D5. IR spectra of the complex **1**.

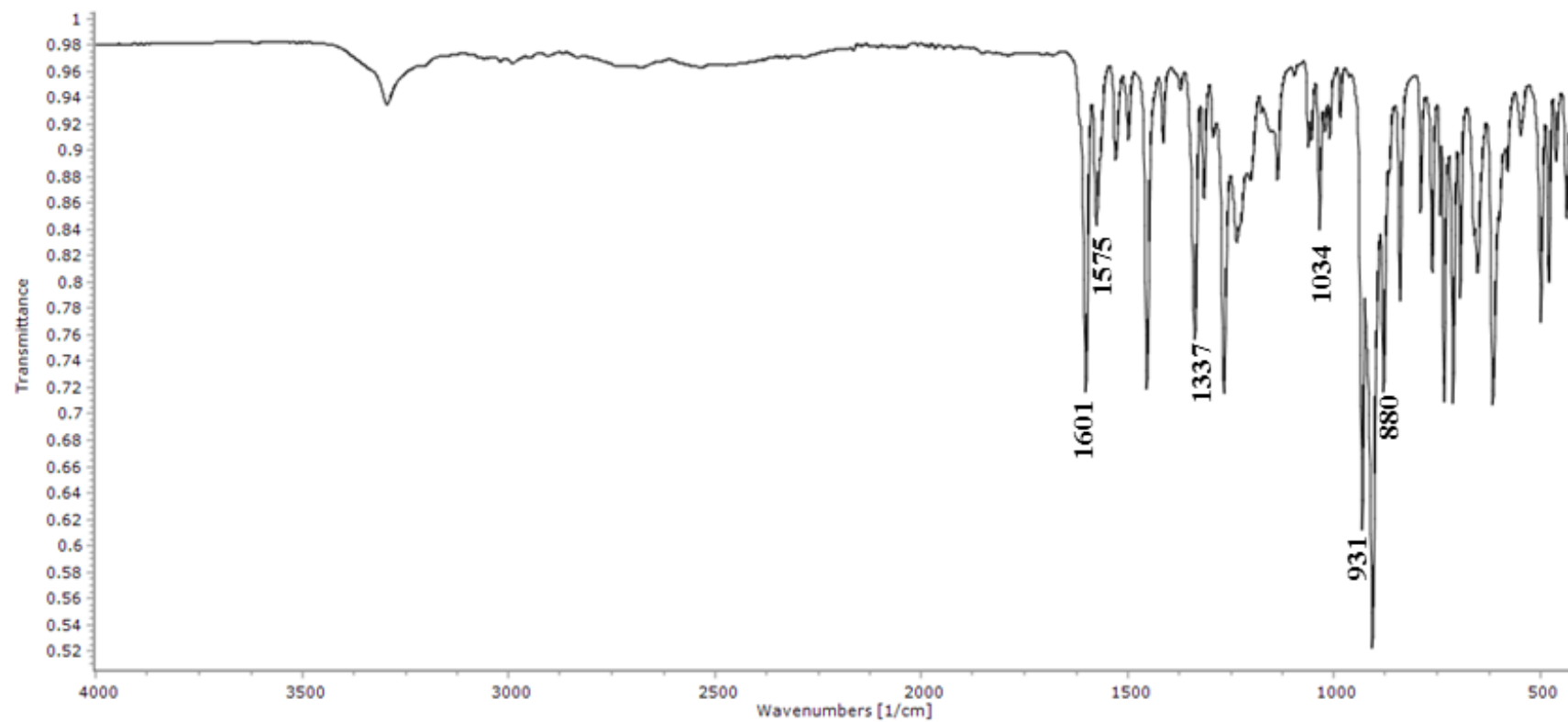Figure D6. IR spectra of the complex **1a** (solution based synthesis).

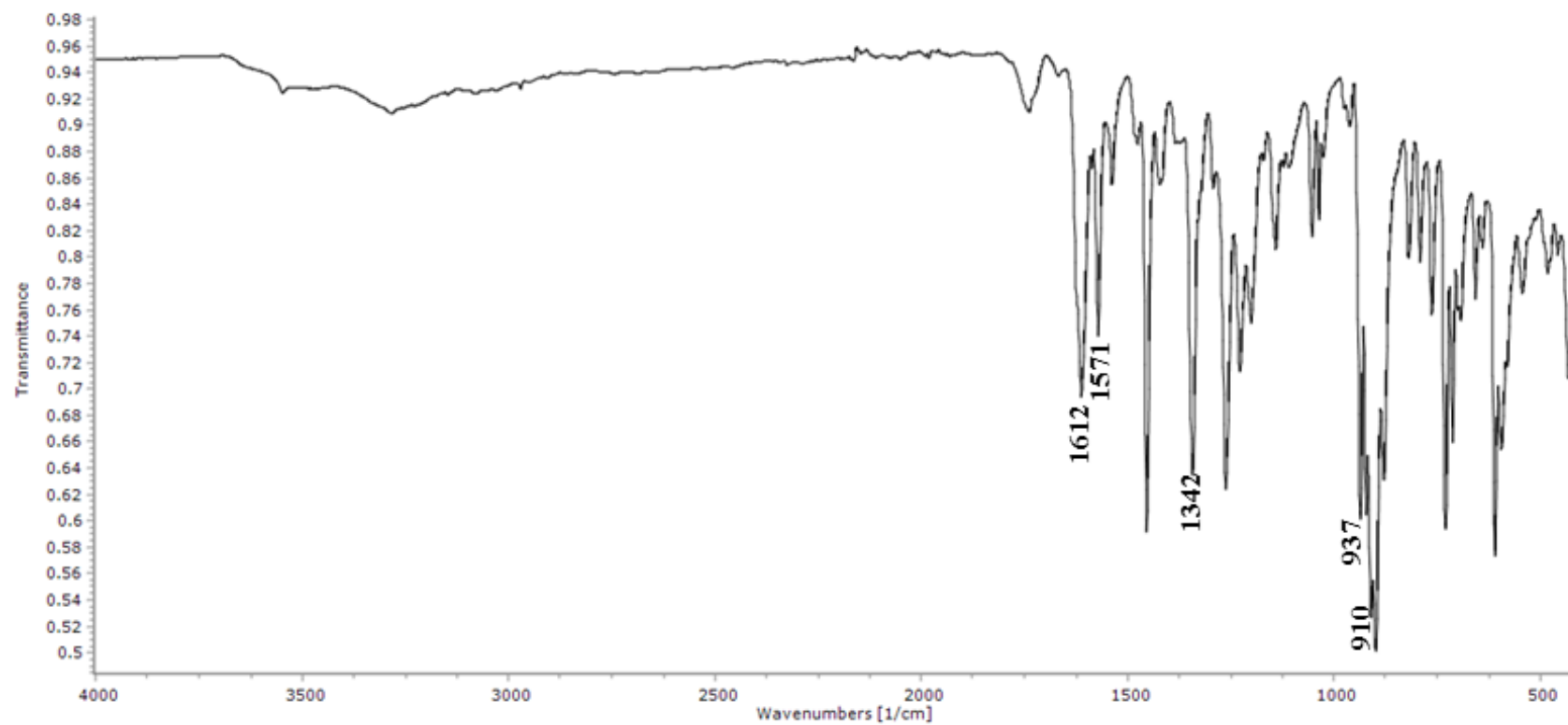Figure D7. IR spectra of the complex **1a** (mechanochemical synthesis).

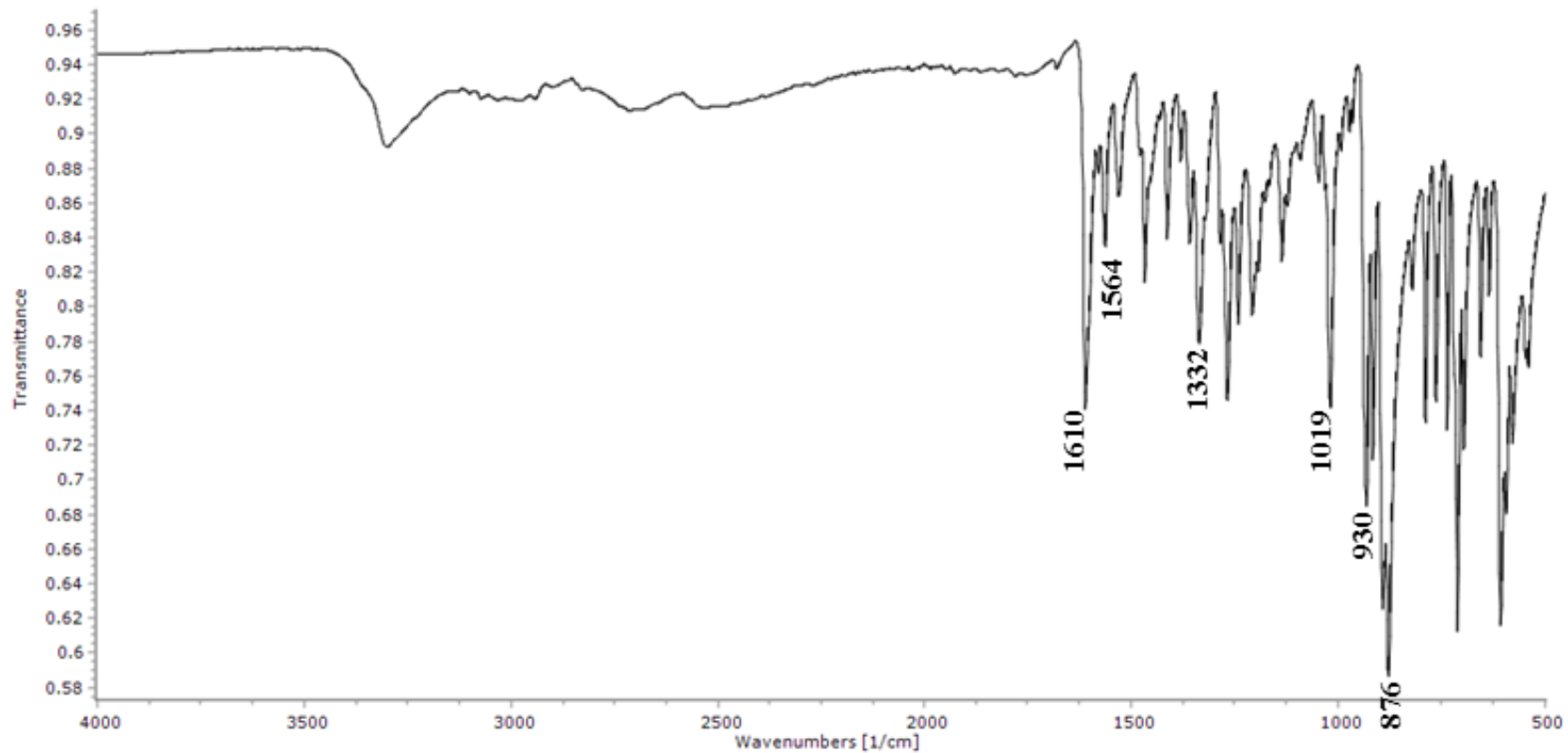Figure D8. IR spectra of the complex **2**.

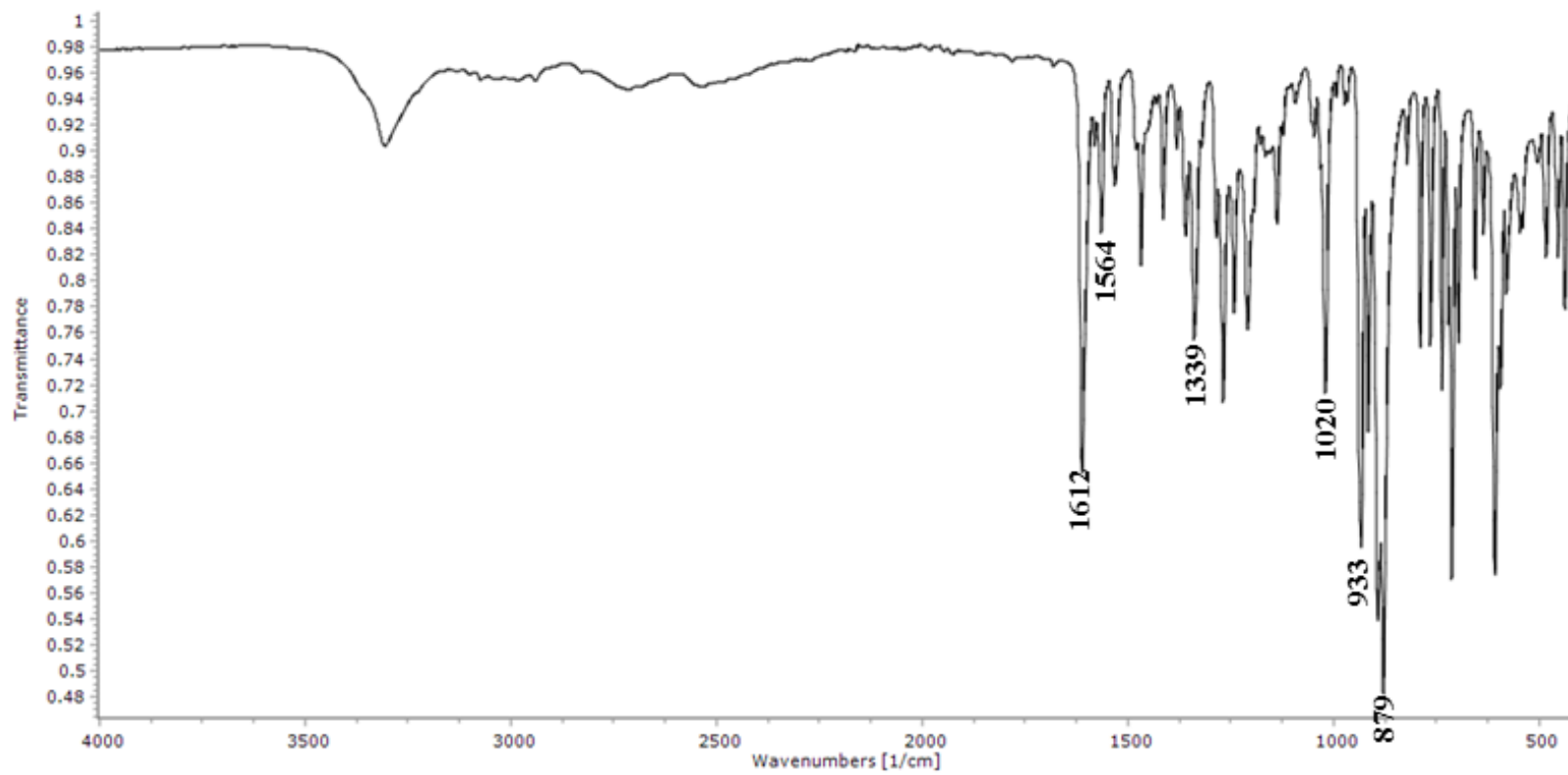Figure D9. IR spectra of the complex **2a** (solution based synthesis).

Figure D10. IR spectra of the complex **2a** (mechanochemical synthesis).

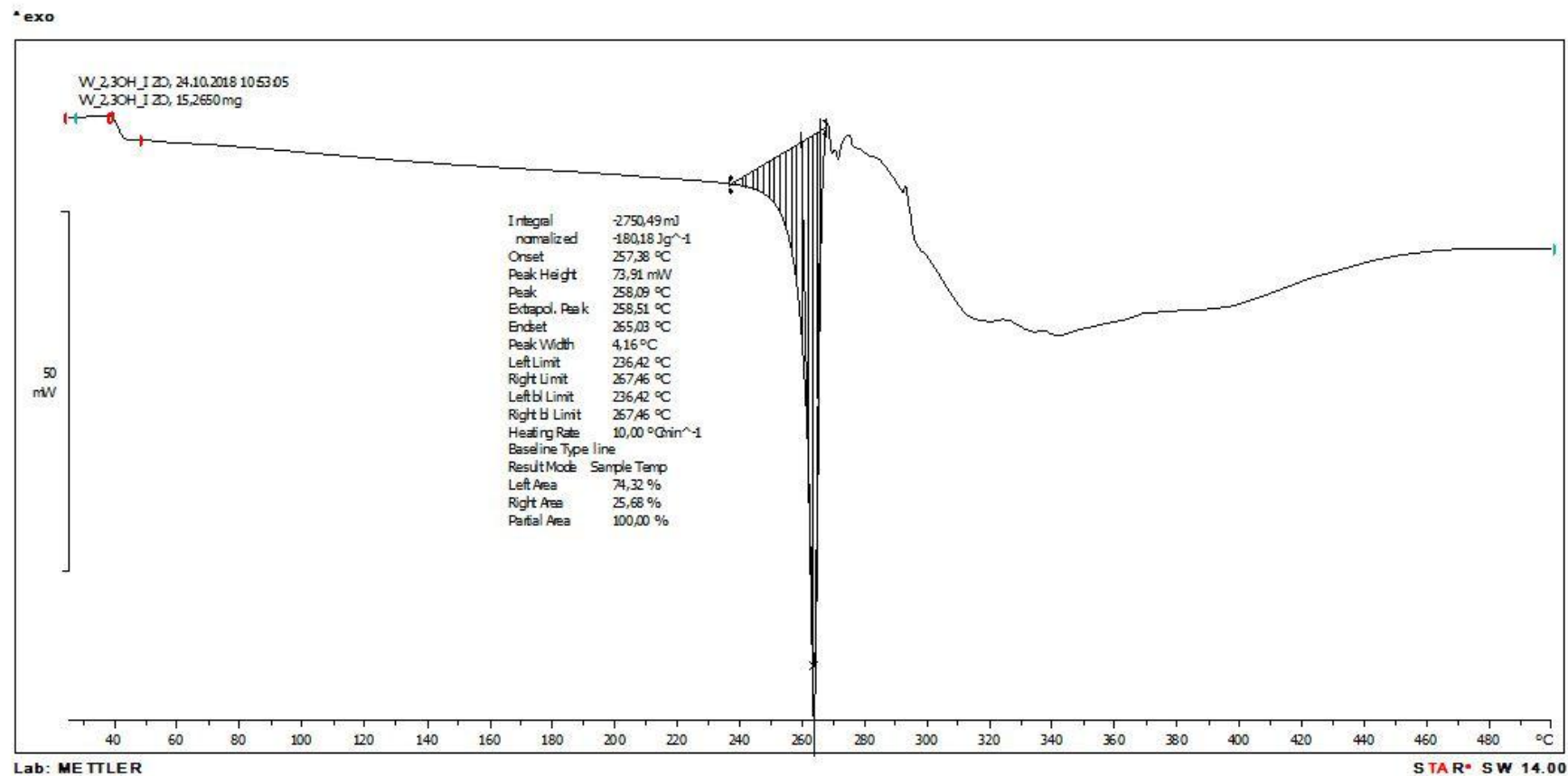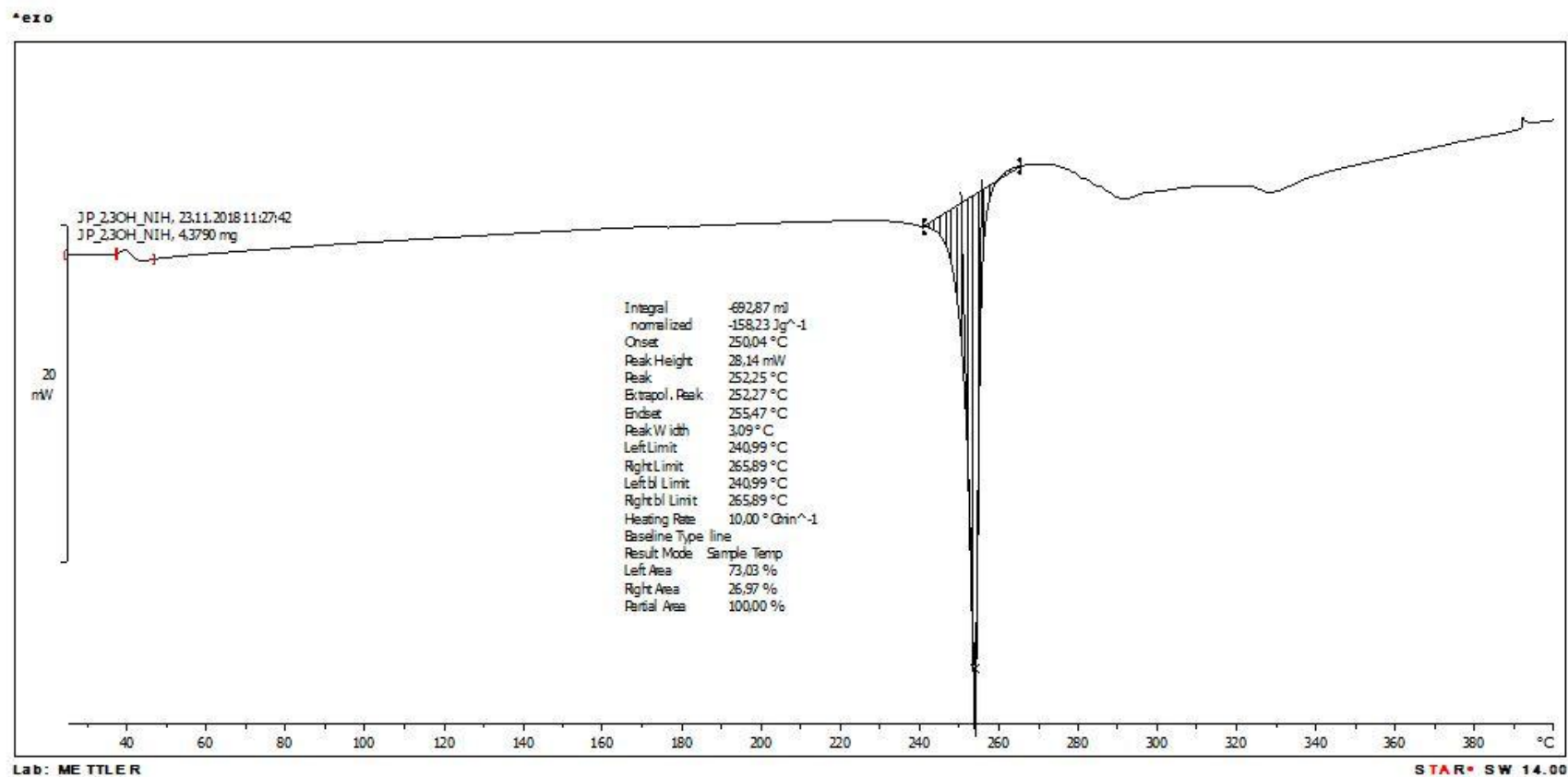Figure D11. DSC curve for ligand $H_2L^1 \cdot MeOH$ after prolonges standing at the room temperature.

Figure D12. DSC curve for ligand H_2L^2.
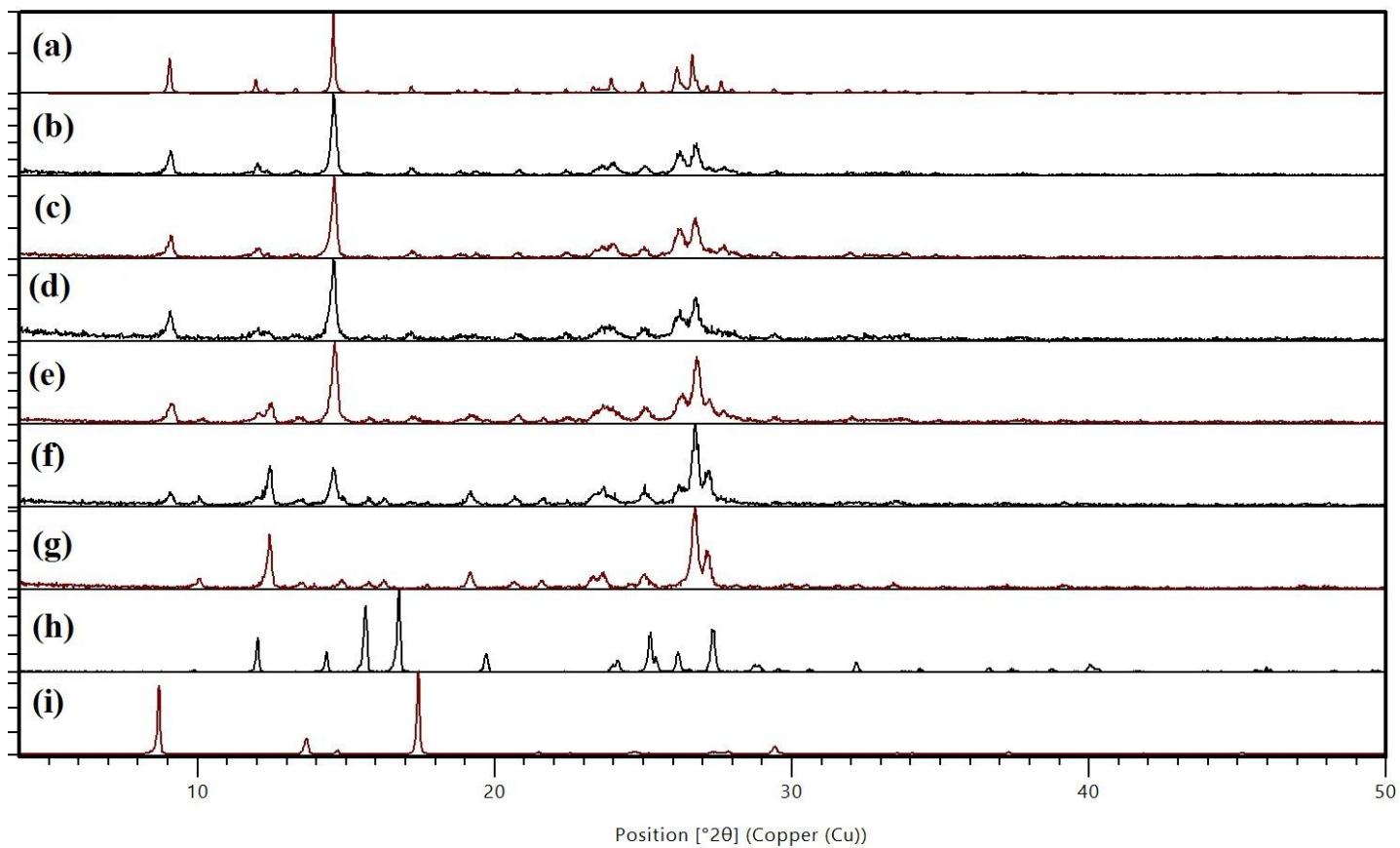
Figure D13. Powder X-ray diffraction patterns of the **H₂L¹** ligands obtained (a) from CCDC database[38] and after (b) 60 min, (c) 50 min, (d) 40 min, (e) 30 min, (f) 20 min, (g) 10 min; and of starting compounds (h) isonicotinic hydrazide (i) 2,3 – dihydroxybenzaldehyde.
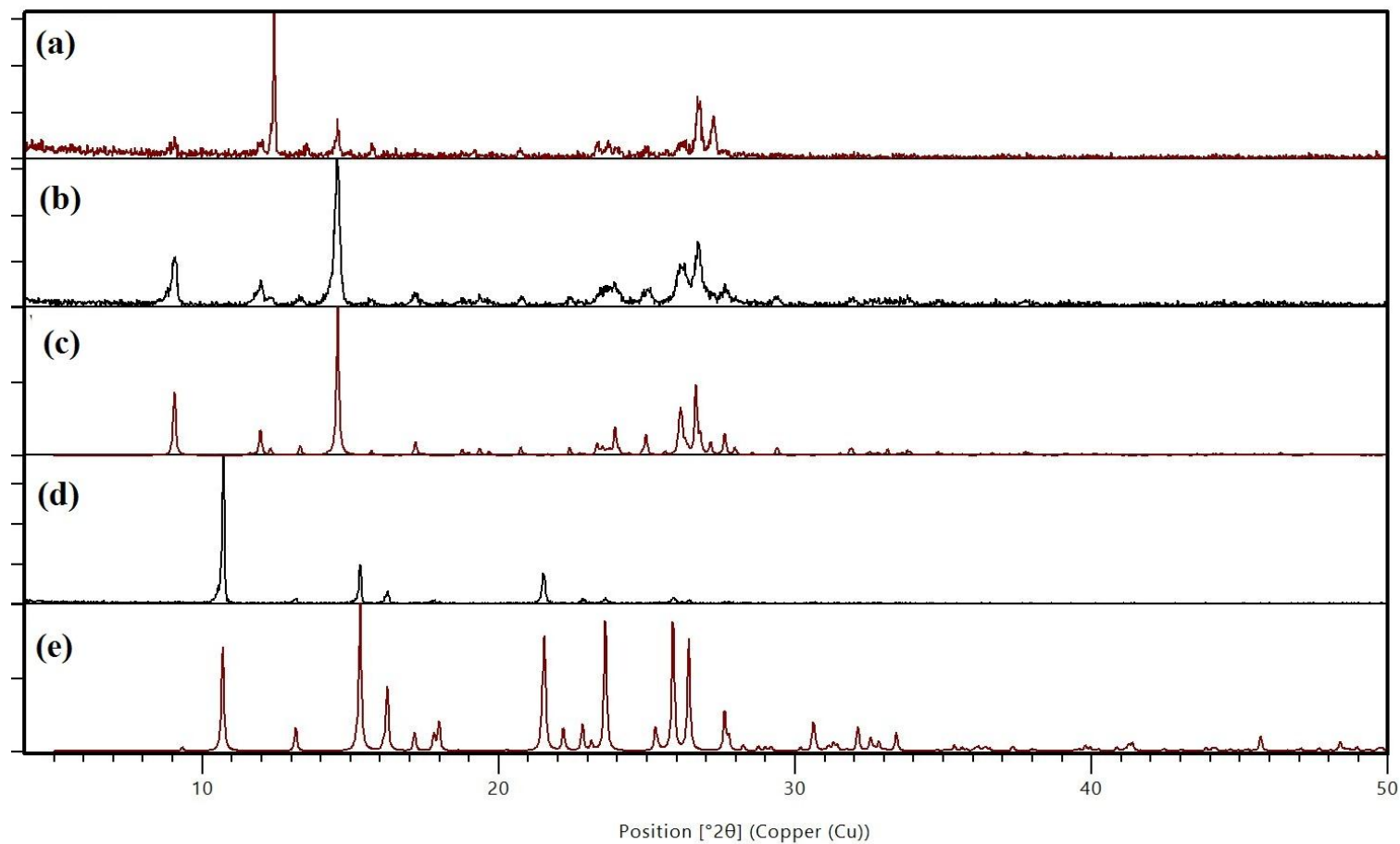
Figure D14. Powder X-ray diffraction patterns of the ligands: (a) **H₂L¹·MeOH** (solution based synthesis), (b) **H₂L¹** (mechanochemical synthesis), (c) **H₂L¹** (CCDC database[38]), (d) **H₂L²**(solution based synthesis) and (e) **H₂L²** (CCDC database[39]).
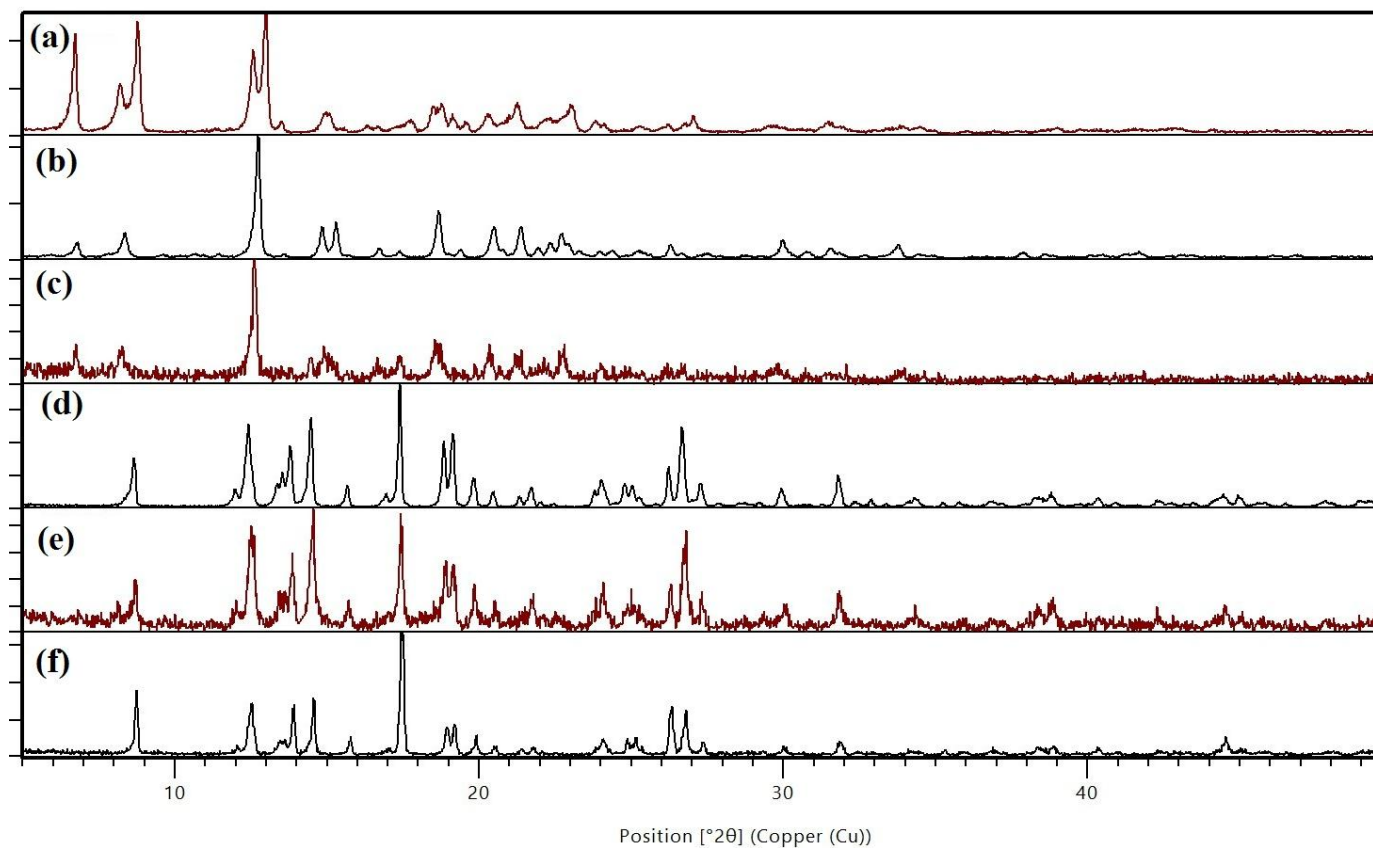
Figure D15. Powder X-ray diffraction patterns of the complexes with **H₂L¹** ligand: (a) **1·MeCN**, (b) **1**, (c) **1** obtained after 2 hours of refluxing of complex **1a** in acetonitrile, (d) **1a** (solution based synthesis), (e) **1a** (mechanochemical synthesis), (f) **1a** obtained after 2 hours of refluxing of complex **1** in methanol.
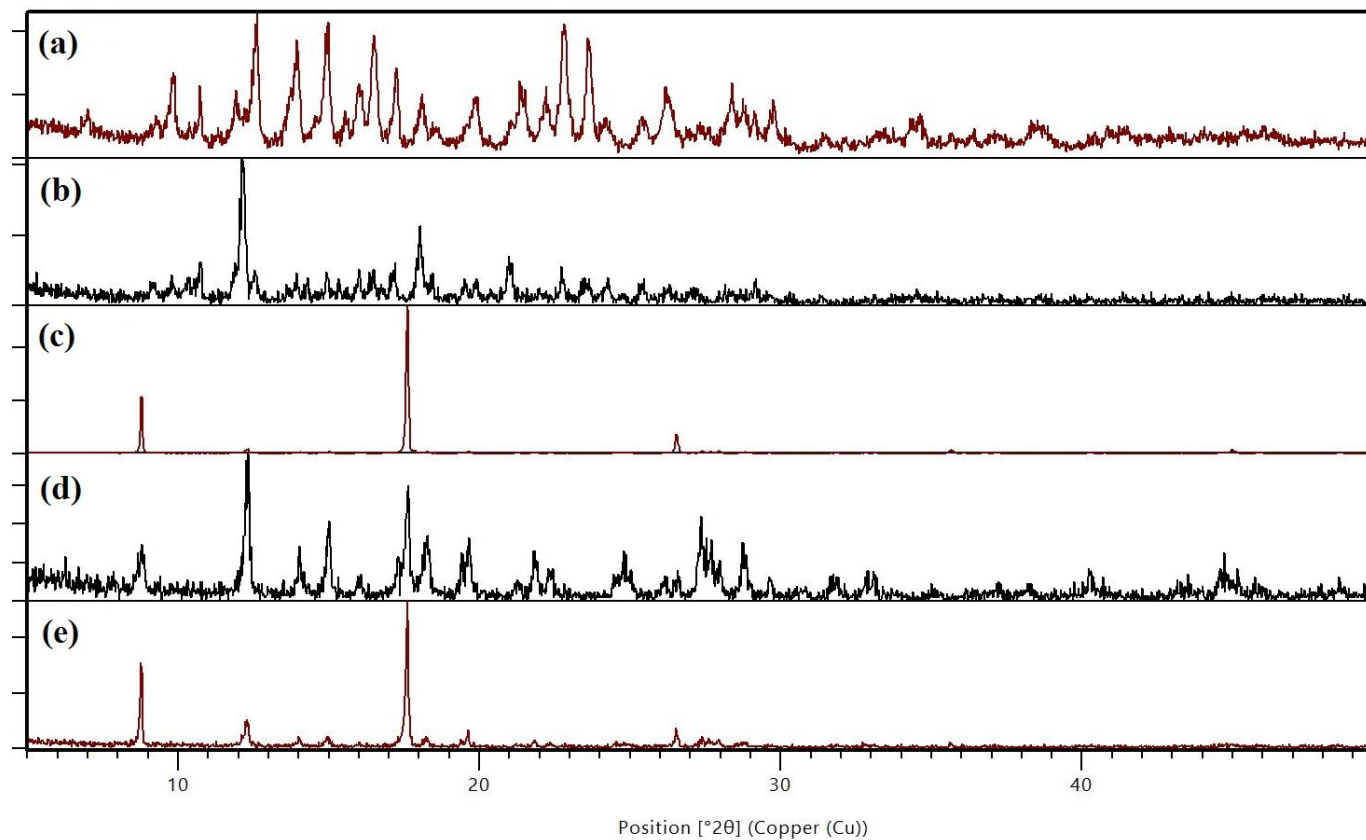
Figure D16. Powder X-ray diffraction patterns of the complexes with H_2L^2 ligand: (a) **2**, (b) **2** obtained after 2 hours of refluxing of complex **2a** in acetonitrile, (c) **2a** (solution based synthesis), (d) **2a** (mechanochemical synthesis), (e) **2a** obtained after 2 hours of refluxing of complex **2** in methanol.
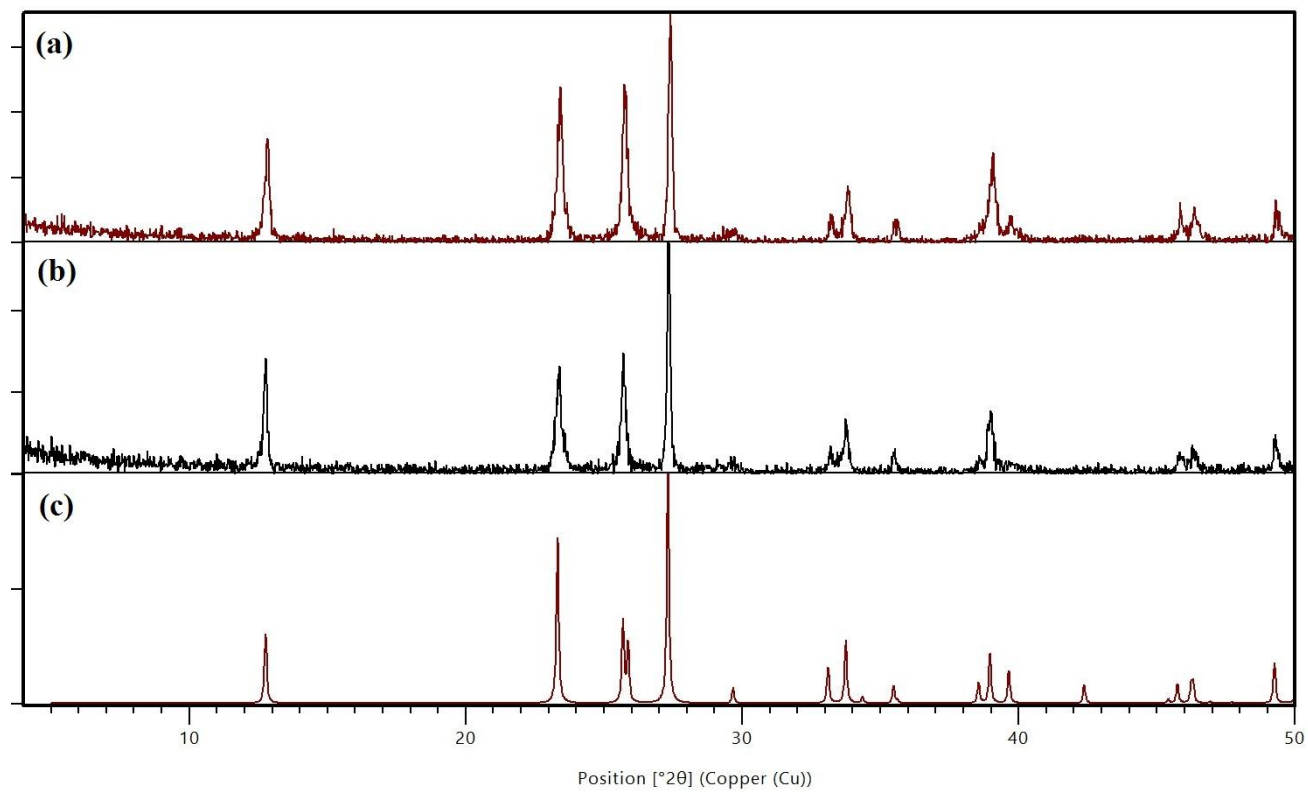
Fig. D17. Powder X-ray diffraction patterns of MoO$_3$ (a) commercially available, (b) residue left after termal decomposition of complex **2,** (c) obtained from database[46].
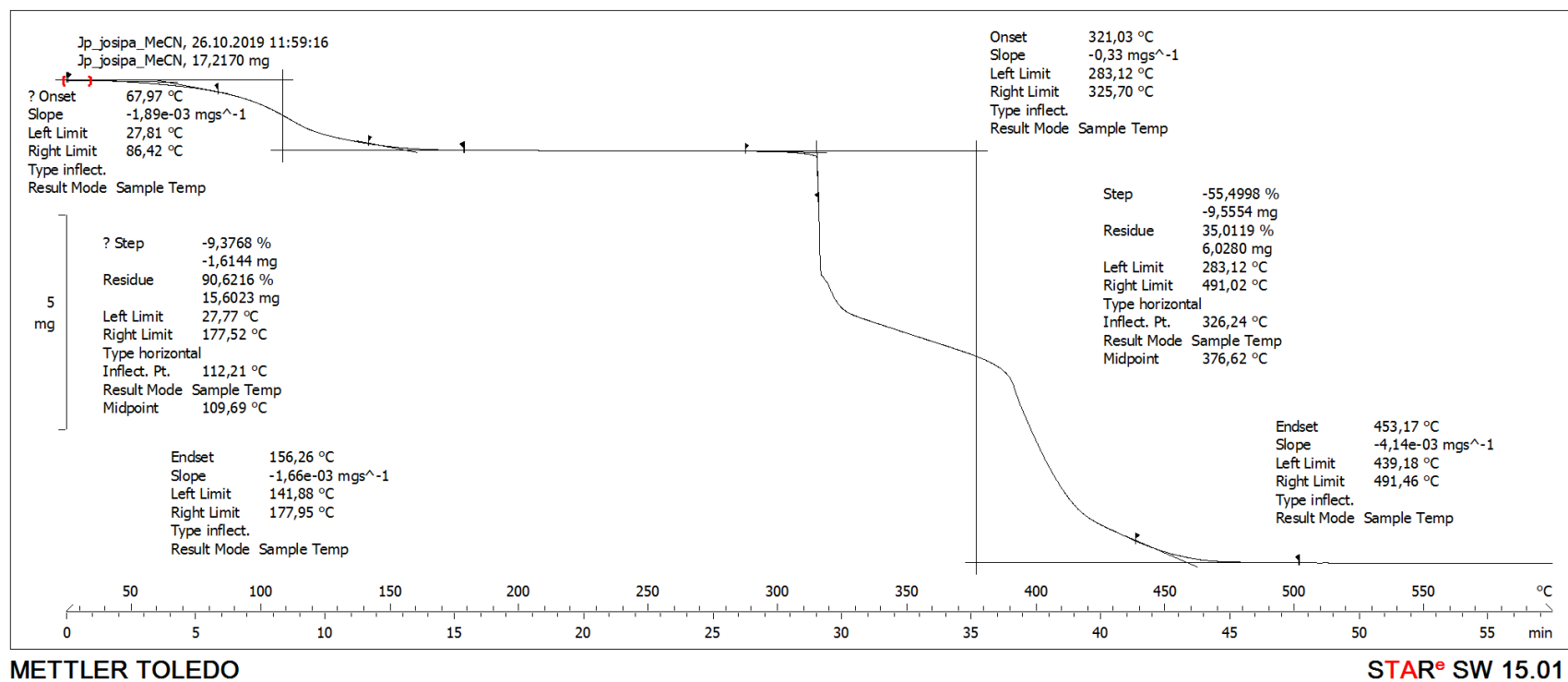
Figure D18. Termogram of the complex **1·MeCN.**

Figure D19. Termogram of the complex **1.**

W_927, 23.09.2019 22:37:08
W_927, 11,0810 mg

Onset 158,88 ℃
Slope -614,34e-06 mgs^-1
Left Limit 131,76 ℃
Right Limit 179,00 ℃
Result Mode Sample Temp

Step -7,5206 %
-0,8334 mg
Residue 92,8224 %
10,2856 mg
Left Limit 131,32 ℃
Right Limit 240,43 ℃
Result Mode Sample Temp

Endset 225,39 ℃
Slope -1,44e-03 mgs^-1
Left Limit 209,34 ℃
Right Limit 239,56 ℃
Result Mode Sample Temp

Onset 306,57 ℃
Slope -16,60e-03 mgs^-1
Left Limit 257,18 ℃
Right Limit 316,94 ℃
Result Mode Sample Temp

Step -57,3774 %
-6,3580 mg
Residue 35,5022 %
3,9340 mg
Left Limit 256,73 ℃
Right Limit 539,82 ℃
Result Mode Sample Temp

Endset 487,37 ℃
Slope -1,89e-03 mgs^-1
Left Limit 459,49 ℃
Right Limit 539,82 ℃
Result Mode Sample Temp

5 mg

METTLER TOLEDO

STAR^e SW 15.01

Figure D20. Termogram of the complex **1a.**

W929, 23.09.2019 22:07:34
W929, 6,1010 mg

Onset 318,15 ºC
Slope -26,71e-03 mgs^-1
Left Limit 197,31 ºC
Right Limit 328,11 ºC
Result Mode Sample Temp

Step -60,4685 %
-3,6892 mg
Residue 37,5029 %
2,2880 mg
Left Limit 196,01 ºC
Right Limit 538,11 ºC
Result Mode Sample Temp

Endset 471,27 ºC
Slope -1,95e-03 mgs^-1
Left Limit 445,76 ºC
Right Limit 539,40 ºC
Result Mode Sample Temp

2 mg

METTLER TOLEDO

STARᵉ SW 15.01

Figure D21. Termogram of the complex **2.**

W911, 23.09.2019 22:45:07
W911, 6,6600 mg

Onset   216,82 °C
Slope   -40,71e-03 mg°C^-1
Left Limit   193,88 °C
Right Limit   222,95 °C
Type inflect.
Result Mode Sample Temp

Step   -7,3321 %
               -0,4883 mg
Residue   93,2810 %
               6,2125 mg
Left Limit   191,32 °C
Right Limit   239,52 °C
Type horizontal
Result Mode Sample Temp

Endset   228,90 °C
Slope   -35,85e-03 mg°C^-1
Left Limit   219,90 °C
Right Limit   237,78 °C
Type inflect.
Result Mode Sample Temp

Onset   313,04 °C
Slope   -0,15 mg°C^-1
Left Limit   266,59 °C
Right Limit   321,36 °C
Type inflect.

Step   -56,9252 %
               -3,7912 mg
Residue   36,1829 %
               2,4098 mg
Left Limit   265,29 °C
Right Limit   518,20 °C
Type horizontal
Result Mode Sample Temp

Endset   475,68 °C
Slope   -10,09e-03 mg°C^-1
Left Limit   460,16 °C
Right Limit   517,33 °C
Type inflect.

2 mg

50   100   150   200   250   300   350   400   450   500   550   °C

METTLER TOLEDO   STAR^e SW 15.01
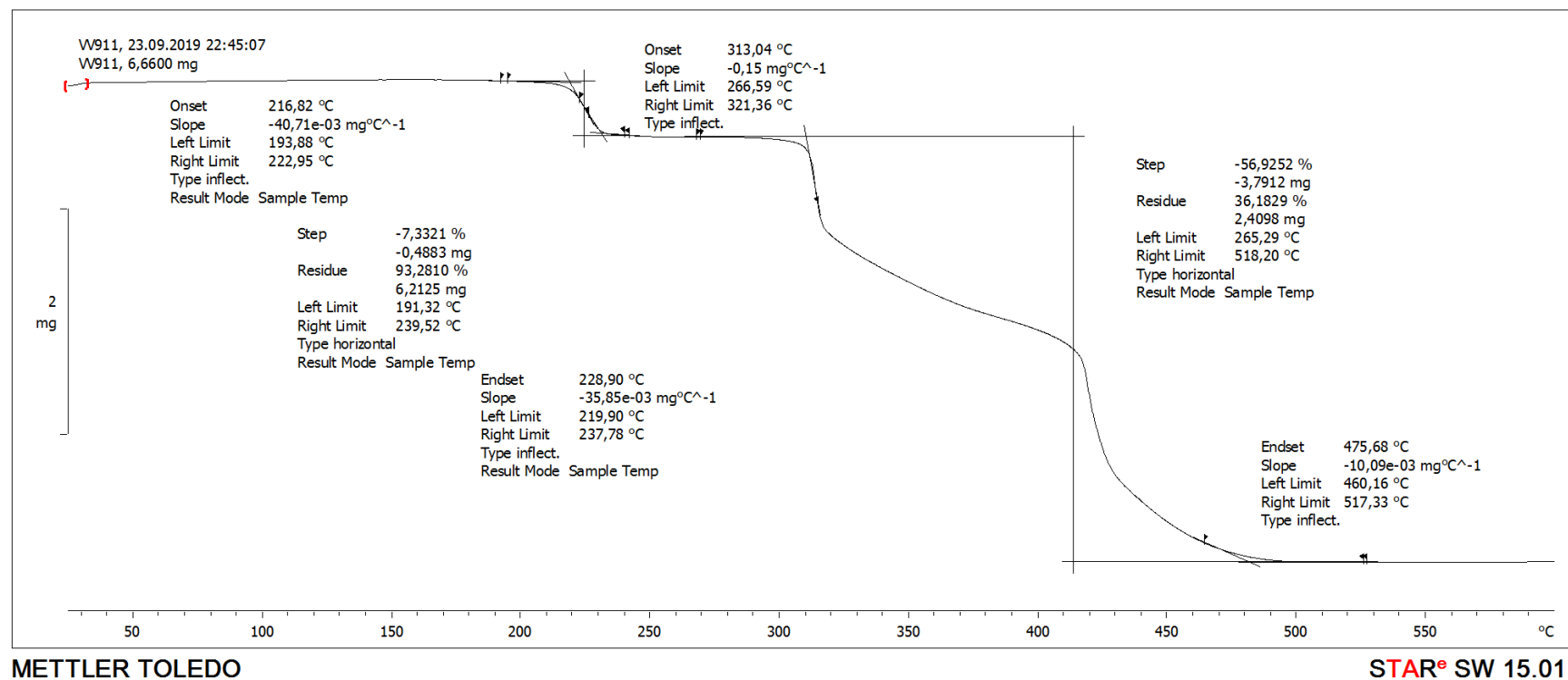
Figure D22. Termogram of the complex **2a.**

Table D1. NMR data of molybdenum(VI) complexes **1** and **2.**

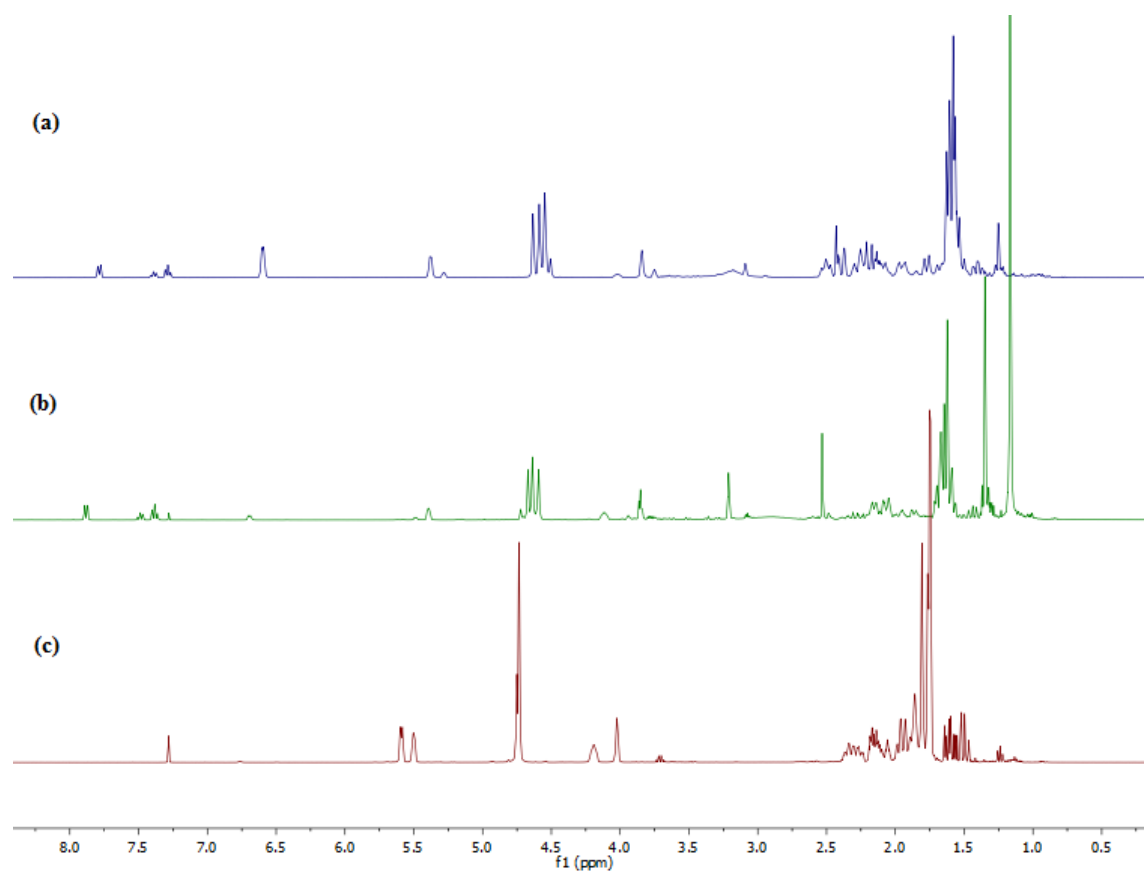| Com	**1**		**2**	
atom	$\delta(^1H)$/ppm	$\delta(^{13}C)$/ppm	$\delta(^1H)$/ppm	$\delta(^{13}C)$/ppm
1		138.05		126.70
2	7.87	121.99	9.15	149.21
3	8.76	151.10	8.76	152.80
4	8.76	151.10	7.56	124.99
5	7.87	121.99	8.31	135.85
6		167.43		167.52
7	8.97	158.24	8.94	157.38
8		121.02		121.09
9		148.69		148.56
10		146.71		146.68
11	7.22	125.16	7.21	124.45
12	6.93	122.38	6.92	122.32
13	7.10	121.90	7.02	121.66
14	9.51		9.49	
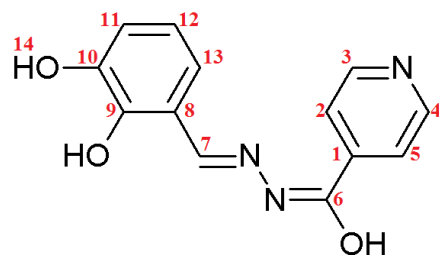
H_2L^1
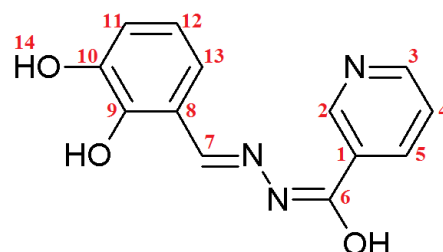
H_2L^2

Figure D23. NMR spectra obtained from reaction mixture (complex **2a**) with (a) aqueous TBHP and (b) H₂O₂, (c) *cis*- and *trans*-

carveol mixture.

§ 9. CURRICULUM VITAE

Personal Information

Name and surname: Josipa Mihalinec

Date of birth: 23. September 1993

Place of birth: Koprivnica

Education

2000–2008	Elementary School Mirko Pereš, Kapela
2008–2012	Gymnasium Bjelovar, Bjelovar
2012–2017	Undergraduate Studies in Chemistry, Faculty of Science, University of Zagreb
2019	Erasmus+ Internship, CNRS-LCC/IUT, Castres

Activities in Popularization of Science

Participation in the organization of Open day of Chemistry